

# Exploring ternary and quaternary mixtures in the **LiBH<sub>4</sub>-NaBH<sub>4</sub>-KBH<sub>4</sub>-Mg(BH<sub>4</sub>)<sub>2</sub>-Ca(BH<sub>4</sub>)<sub>2</sub> system**

Erika M. Dematteis,<sup>a)b)</sup> Claudio Pistidda,<sup>b)</sup> Martin Dornheim<sup>b)</sup> and Marcello Baricco<sup>a)\*</sup>

<sup>a)</sup>Department of Chemistry and Inter-departmental Center Nanostructured Interfaces and Surfaces (NIS), University of Turin, Via Pietro Giuria 7, 10125 Torino, Italy

<sup>b)</sup>Nanotechnology Department, Helmholtz-Zentrum Geesthacht Max-Planck Straße 1, 21502, Geesthacht, Germany

\*Corresponding author

Marcello Baricco

E-mail address: marcello.baricco@unito.it

Tel.: +39 011 6707569

Fax: +39 0116707856

## Abstract

Binary combinations of borohydrides have been extensively investigated evidencing the formation of eutectics, bimetallic compounds or solid solutions. In this paper, the investigation has been extended to ternary and quaternary systems in the  $\text{LiBH}_4\text{-NaBH}_4\text{-KBH}_4\text{-Mg}(\text{BH}_4)_2\text{-Ca}(\text{BH}_4)_2$  system. Possible interactions among borohydrides in equimolar composition has been explored by mechanochemical treatment. The obtained phases were analysed by X-ray diffraction and the thermal behaviour of the mixtures were analysed by HP-DSC and DTA, defining temperature of transitions and decomposition reactions. The release of hydrogen was detected by MS, showing the role of the presence of solid solutions and multi-cation compounds on the hydrogen desorption reactions. The presence of  $\text{LiBH}_4$  generally promotes the release of  $\text{H}_2$  at about  $200\text{ }^\circ\text{C}$ , while  $\text{KCa}(\text{BH}_4)_3$  promotes the release in a single-step reaction at higher temperatures.

The explorative investigation has evidenced the formation of bi/tri-metallic compounds such as  $\text{KCa}(\text{BH}_4)_3$ ,  $\text{LiKMg}(\text{BH}_4)_4$  and  $\text{LiK}(\text{BH}_4)_2$ . The relative thermodynamic stabilities of these compounds have been discussed in the present study. Many new ternary eutectics have been observed with a melting temperature in the range from  $100\text{ }^\circ\text{C}$  to  $140\text{ }^\circ\text{C}$ , much lower than the melting temperature of parent binary eutectics. The hydrogen desorption occurs from the liquid phase, via complex multi-steps reactions but with no significant differences compared to the quinary equimolar mixture previously investigated.

**Keywords:** complex hydrides, borohydride, ternary, quaternary, hydrogen storage.

## Introduction

In the  $\text{LiBH}_4\text{-NaBH}_4\text{-KBH}_4\text{-Mg}(\text{BH}_4)_2\text{-Ca}(\text{BH}_4)_2$  system, pure borohydrides compounds and some bimetallic or trimetallic compounds have been extensively studied in the literature.[1] Solubility of borohydrides in solid and liquid phases has been recently reviewed and discussed, underling a limited interaction in solid phases and extensive solubility in the liquid phase.[2]

Pure borohydrides are characterised by different crystal structures and coordination and they all present a polymorphic transition from a low temperature structure to a high temperature polymorph, followed by melting and release of hydrogen at higher temperatures.[1],[3],[4],[5],[6],[7],[8],[9],[10]

Binary combinations of borohydrides evidence the formation of eutectics, bimetallic compounds or solid solutions. Details on binary experimental studies reported in the literature have been summarized by the present author in ref.[11]. Many eutectics are formed at a different molar fraction composition, from a temperature as low as 105 °C for 0.725 $\text{LiBH}_4$ -0.275 $\text{KBH}_4$ , [12],[13] 216 °C for 0.70 $\text{LiBH}_4$ -0.30 $\text{NaBH}_4$ , [14],[15] 150 °C for 0.55 $\text{LiBH}_4$ -0.45 $\text{Mg}(\text{BH}_4)_2$ , [16],[17],[18], and 200 °C for 0.68 $\text{LiBH}_4$ -0.32 $\text{Ca}(\text{BH}_4)_2$ . [19],[20] In binary combinations without  $\text{LiBH}_4$ , thermal minima or partial melting have been observed, at 462 °C for 0.682 $\text{NaBH}_4$ -0.328 $\text{KBH}_4$ , [21] 205 °C for 0.40 $\text{NaBH}_4$ -0.60 $\text{Mg}(\text{BH}_4)_2$ , [22] and above 350°C for the  $\text{NaBH}_4\text{-Ca}(\text{BH}_4)_2$  system. [22] The formation of solid solutions is limited to the  $\text{NaBH}_4\text{-KBH}_4$  [21] and  $\text{LiBH}_4\text{-NaBH}_4$  [14] systems. Furthermore, when  $\text{KBH}_4$  is mixed with other borohydrides, it forms bimetallic compound such as  $\text{K}_2\text{Mg}(\text{BH}_4)_4$ ,  $\text{K}_3\text{Mg}(\text{BH}_4)_5$ , [23] and  $\text{KCa}(\text{BH}_4)_3$ . [24] However, their binary systems were not investigated as a function of temperature and composition. Finally, the  $\text{Mg}(\text{BH}_4)_2\text{-Ca}(\text{BH}_4)_2$  system have never been experimentally investigated as a function of composition and temperature, but a study is undergoing from the present authors. [25]

Among ten possible ternary combinations, only the  $\text{LiBH}_4\text{-NaBH}_4\text{-KBH}_4$  system have been characterized experimentally in details and assessed by the Calphad method, revealing a ternary

eutectic at 103 °C.[6] Few details have been reported on the  $\text{LiBH}_4\text{-KBH}_4\text{-Mg}(\text{BH}_4)_2$  system in the literature,[26] reporting the formation of  $\text{LiKMg}(\text{BH}_4)_4$  and  $\text{Li}_2\text{K}_3\text{Mg}_2(\text{BH}_4)_9$  trimetallic compounds, while no interactions have been observed in the  $\text{LiBH}_4\text{-KBH}_4\text{-Ca}(\text{BH}_4)_2$  system.[27]

Possible quaternary combinations in the system are five and they have not been explored yet. Recently, a quinary equimolar mixture of  $\text{LiBH}_4\text{-NaBH}_4\text{-KBH}_4\text{-Mg}(\text{BH}_4)_2\text{-Ca}(\text{BH}_4)_2$  was investigated by the present authors, evidencing, for the first time, the formation of a liquid borohydride with five different cations.[11] While the mixing among borohydrides in the liquid phase seems to suggest a negative enthalpy of mixing, interactions in the solid phases bring to the formation of  $\text{KCa}(\text{BH}_4)_3$  bimetallic compound, but no significant solubility is observed.

The occurrence of solid solutions, multi-cation eutectics and multi-metallic compounds leads to differences in the hydrogen desorption reactions, depending on the interaction among the components. For instance, the occurrence of a liquid phase enable easy tailoring of the decomposition temperature of borohydrides by both nanoconfinement[28],[29] and in mixture with reactive hydride composites.[30],[31] The presence of a liquid phase in reactive hydride composites, provides a synergic effect in improving hydrogen release and cyclability.[32],[33] Improvements in hydrogen release properties in these systems are usually related to interfaces and microstructures, where the liquid phase promotes local contact between boundaries of the complex hydrides in the mixture.[34],[35],[36],[37] Generally, in binary and ternary systems with the formation of eutectics, the hydrogen release occurs involving a liquid phase, usually above 200 °C as evidenced by Paskevicious et al.[38]. The  $\text{KCa}(\text{BH}_4)_3$  bimetallic compound formed in the quinary system also plays a role in decomposition processes.[11]

Decomposition reactions and hydrogen release from eutectic borohydrides, are occurring in some cases at high temperature, i.e. the  $\text{LiK}$  and  $\text{LiNa}$  eutectics decompose above 400 °C.[12],[15], however they can be easily lowered to 250 °C when nanoconfined.[39] Decomposition of  $\text{LiMg}$  and  $\text{LiCa}$  eutectics occur above 250 °C and 350°C respectively.[16],[17],[18],[19] The

nanoconfinement improved these reactions lowering the hydrogen release temperature to 150 °C and 200 °C respectively.[40],[41],[42],[43],[44],[45]

Since only few ternary systems have been explored in the literature, while no quaternaries have never been investigated, the present study aims to investigate mixtures in the  $\text{LiBH}_4\text{-NaBH}_4\text{-KBH}_4\text{-Mg}(\text{BH}_4)_2\text{-Ca}(\text{BH}_4)_2$  system. The goal is to explore equimolar compositions in ternary and quaternary combinations, synthesized by mechanochemical treatment, and to study their thermal behaviour as function of temperature to further explore and understand possible interactions among borohydrides and their role in improving hydrogen release properties.

The mixtures were synthesized from commercial  $\text{LiBH}_4$ ,  $\text{NaBH}_4$ ,  $\text{KBH}_4$ ,  $\gamma\text{-Mg}(\text{BH}_4)_2$  and  $\alpha,\beta\text{-Ca}(\text{BH}_4)_2$ . The obtained phases were analysed at room temperature by X-ray diffraction to define the obtained crystal phases after ball milling and after thermal treatment up to 200 °C. HP-DSC and DTA-MS were used to study the thermal behaviour of the mixture, defining temperature of transitions and decomposition reactions.

## **Experimental**

### ***Sample preparation***

Lithium borohydride ( $\text{LiBH}_4$ , purity >95% from Sigma-Aldrich), sodium borohydride ( $\text{NaBH}_4$ , purity >98% from ABCR), potassium borohydride ( $\text{KBH}_4$ , purity >97% from Merck), magnesium borohydride ( $\gamma\text{-Mg}(\text{BH}_4)_2$ , purity >95% from Sigma Aldrich) and calcium borohydride (mixed  $\alpha$ - and  $\beta\text{-Ca}(\text{BH}_4)_2$ , purity >99% from KatChem) were mixed by ball milling (BM) in equimolar ratio. For the sake of brevity, mixtures will be named listing the constituent metals. A planetary mill (Fritsch Pulverisette 6) was used to mix the reactants under 10 bar of  $\text{H}_2$  in 250 mL stainless steel vials with stainless steel balls (o.d. 10 mm) and a balls-to-sample mass ratio of 30:1. The pure borohydrides in the correct composition ratio were milled continually for 1 h at 350 r.p.m. A thermal treatment of ball-milled samples was performed in a glass capillary placed in a quartz tube under inert gas, using an oil bath heated at 200 °C. All preparations and manipulations of the

samples were performed in an argon-filled or nitrogen-filled glove boxes with a circulation purifier,  $p(\text{O}_2, \text{H}_2\text{O}) < 1$  ppm.

### ***Powder X-ray diffraction (PXD)***

Powder X-ray diffraction (PXD) measurements were performed at room temperature using a Panalytical X-pert (Cu  $K_\alpha = 1.54059$  Å,  $K_\beta = 1.54446$  Å) in capillary transmission set-up (Debye-Scherrer geometry). Patterns were collected from  $5^\circ$  to  $130^\circ$   $2\theta$  range, step size 0.016, time step 90 seconds. Samples were mounted in the glove box in 0.5 mm glass capillaries and sealed with plastiline, then moved out of the glove box and sealed with flame.

### ***High Pressure Differential scanning calorimetry (HP-DSC)***

A high-pressure 204 Netsch DSC (HP-DSC) was used to analyse the thermal behaviour of the mixture avoiding decomposition and obtaining accurate values of temperature of phase transformations. The instrument is placed inside a glove box to ensure sample handling under inert atmosphere. Approximately 3 to 9 mg of sample were loaded into aluminium crucibles with lid. Samples were heated and cooled in the desired temperature range at  $5^\circ\text{C}/\text{min}$  under 1 bar of  $\text{H}_2$ .

### ***Differential Temperature Analysis coupled with Mass Spectroscopy (DTA-MS)***

A DTA Netzsch STA 409 coupled with a Hiden Analytical Hal 201 Mass Spectrometer (MS) was used to analyse hydrogen and diborane release in the mixture as a function of temperature. The instrument is placed inside a glove box to ensure sample handling under inert atmosphere. Approx. 2 mg of sample were heated from room temperature up to  $500^\circ\text{C}$  at  $5^\circ\text{C}/\text{min}$  under an argon gas flow of 50 mL/min, which was used also to transport the gases to the MS analyser.

## **Results**

### **Ternary Systems**

#### ***LiBH<sub>4</sub>-NaBH<sub>4</sub>-Mg(BH<sub>4</sub>)<sub>2</sub>***

After ball milling, the LiNaMg system (**Figure 1, A**) presents all the starting materials, the  $\gamma$ -Mg(BH<sub>4</sub>)<sub>2</sub> has partially converted into the  $\alpha$  polymorph upon milling (**Figure 1, B, BM**). After the

annealing (**Figure 1, B, 200 °C**), the intensity of the  $\text{Mg}(\text{BH}_4)_2$  PXD peaks is decreasing, the  $\gamma$ -phase is no more present while PXD peaks from the  $\beta$ -phase can be recognised. Some broad PXD peaks can be detected, indicating a possible reaction of  $\text{Mg}(\text{BH}_4)_2$  to form not crystalline compounds at higher temperature as previously reported in the literature.[46],[47] In **Figure 1, C**, from the HP-DSC analysis, two main reversible phase transitions can be observed. The first peak at  $T_{\text{peak}} = 99 \text{ °C}$  ( $86 \text{ °C}$ , on cooling) is related to the phase transition (PT) of  $\text{LiBH}_4$ , observed at a temperature lower than that of the pure compound because of the presence of an orthorhombic solid solution with  $\text{NaBH}_4$ . [14] The second peak at  $T_{\text{peak}} = 145 \text{ °C}$  ( $135 \text{ °C}$ , on cooling) can be assigned to a new ternary eutectic, while the liquidus temperature is detected around  $160 \text{ °C}$ . In the  $\text{LiNaMg}$  system, hydrogen release is observed at  $T_{\text{peak}} = 276 \text{ °C}$  and  $365 \text{ °C}$  (**Figure 1, D**).

#### ***LiBH<sub>4</sub>-NaBH<sub>4</sub>-Ca(BH<sub>4</sub>)<sub>2</sub>***

If  $\text{Mg}(\text{BH}_4)_2$  is replaced by  $\text{Ca}(\text{BH}_4)_2$ , in the  $\text{LiNaCa}$  system (**Figure 2, A**) no reactions occur upon milling nor annealing. In fact,  $\text{LiBH}_4$ ,  $\text{NaBH}_4$  and  $\alpha\text{-Ca}(\text{BH}_4)_2$  are still present in the PXD pattern (**Figure 2, B, BM and 200 °C**). The HP-DSC trace confirms that no interactions occur upon cycling, as previously reported in the literature.[48] The observed peak is related to the PT of  $\text{LiBH}_4$  at  $T_{\text{peak}} = 99 \text{ °C}$  ( $81 \text{ °C}$ , on cooling) (**Figure 2, C**). On the second cycle, the peak seems to present multiple transitions, which can be related to multiple melting events. The  $\text{LiNaCa}$  system releases hydrogen at a temperature corresponding to that of pure  $\text{Ca}(\text{BH}_4)_2$  and of eutectic with  $\text{LiBH}_4$  and  $\text{Ca}(\text{BH}_4)_2$  ( $T_{\text{peak}} = 361 \text{ °C}$ ,  $378 \text{ °C}$  and  $470 \text{ °C}$ , **Figure 2, D**). [19],[20]

#### ***LiBH<sub>4</sub>-KBH<sub>4</sub>-Mg(BH<sub>4</sub>)<sub>2</sub>***

The  $\text{LiKMg}$  system (**Figure 3, A**) was already studied in the literature.[49] In the present milling conditions, the formation of  $\text{LiKMg}(\text{BH}_4)_4$  and  $\text{LiK}(\text{BH}_4)_2$  compounds has been observed, together with residual  $\text{LiBH}_4$ ,  $\text{KBH}_4$ ,  $\gamma\text{-Mg}(\text{BH}_4)_2$  and  $\alpha\text{-Mg}(\text{BH}_4)_2$  (**Figure 3, B, BM**). Upon cycling in HP-DSC (**Figure 3, C**), the PT of the  $\text{LiBH}_4$  can be observed at  $T_{\text{peak}} = 95 \text{ °C}$ , followed by a double peak, related to the solid-melt reaction to form  $\text{Li}_2\text{K}_3\text{Mg}_2(\text{BH}_4)_9$  described by Schouwink et al..[49] In this reaction,  $\text{LiKMg}(\text{BH}_4)_4$  and  $\text{LiK}(\text{BH}_4)_2$  form  $\text{Li}_2\text{K}_3\text{Mg}_2(\text{BH}_4)_9$ , and then the reaction is

followed by the melting of the eutectic  $\text{LiBH}_4\text{-KBH}_4$ , as confirmed by our HP-DSC analysis at  $T_{\text{peak}} = 103\text{ }^\circ\text{C}$  and  $107\text{ }^\circ\text{C}$ , respectively ( $65\text{ }^\circ\text{C}$ , on cooling). In fact, after annealing (**Figure 3, B, 200**  $^\circ\text{C}$ ) the intensity of PXD peaks of the  $\text{LiKMg}(\text{BH}_4)_4$  compound are more intense, while peaks from  $\text{LiBH}_4$ ,  $\text{KBH}_4$ ,  $\gamma\text{-Mg}(\text{BH}_4)_2$ ,  $\alpha\text{-Mg}(\text{BH}_4)_2$  and  $\text{LiK}(\text{BH}_4)_2$  decreases and almost disappears, underling a not complete reaction to form the trimetallic compound upon milling. The  $\text{LiKMg}$  system releases hydrogen at  $T_{\text{peak}} = 311\text{ }^\circ\text{C}$  and  $390\text{ }^\circ\text{C}$ , because of the decomposition of the trimetallic compound. No further melting reaction seems to be involved at higher temperatures (**Figure 3, D**).[26],[49]

#### ***LiBH<sub>4</sub>-KBH<sub>4</sub>-Ca(BH<sub>4</sub>)<sub>2</sub>***

In the  $\text{LiKCa}$  system (**Figure 4, A**), the formation of the bimetallic  $\text{KCa}(\text{BH}_4)_3$  has been observed after BM, together with a small amount of  $\text{LiBH}_4$  and  $\text{KBH}_4$  phases (**Figure 4, B, BM**), which decrease and almost disappear after annealing (**Figure 4, B, 200**  $^\circ\text{C}$ ). From the HP-DSC trace (**Figure 4, C**), at  $T_{\text{peak}} = 75\text{ }^\circ\text{C}$  ( $68\text{ }^\circ\text{C}$  on cooling) the PT of  $\text{KCa}(\text{BH}_4)_3$  can be recognised, which is more intense and sharp on the second cycle. At  $T_{\text{peak}} = 106\text{ }^\circ\text{C}$  ( $96\text{ }^\circ\text{C}$  on cooling) and  $T_{\text{peak}} = 113\text{ }^\circ\text{C}$  ( $107\text{ }^\circ\text{C}$  on cooling) the PT of  $\text{LiBH}_4$  and eutectic melting of  $\text{LiBH}_4\text{-KBH}_4$  occur, respectively. A liquidus temperature is detected at  $177\text{ }^\circ\text{C}$  ( $170\text{ }^\circ\text{C}$  on cooling), which could be an indication of a possible new ternary eutectic. In fact, no PT of  $\text{Ca}(\text{BH}_4)_2$  is observed, because the compound is present in the liquid state or it is involved in the bimetallic compound, which is also melting in the eutectic reaction. The  $\text{LiKCa}$  system releases hydrogen from the liquid state, at  $T_{\text{peak}} = 343\text{ }^\circ\text{C}$  and  $471\text{ }^\circ\text{C}$  (**Figure 4, D**).

#### ***LiBH<sub>4</sub>-Mg(BH<sub>4</sub>)<sub>2</sub>-Ca(BH<sub>4</sub>)<sub>2</sub>***

In the  $\text{LiMgCa}$  system,  $\text{LiBH}_4$  is combined with two alkaline-earth borohydrides (**Figure 5, A**). After BM, no reactions occur and  $\text{LiBH}_4$ ,  $\gamma\text{-Mg}(\text{BH}_4)_2$ ,  $\alpha\text{-Mg}(\text{BH}_4)_2$  and  $\alpha\text{-Ca}(\text{BH}_4)_2$  phases are observed in the PXD pattern (**Figure 5, B, BM**). Nevertheless, after annealing (**Figure 5, B, 200**  $^\circ\text{C}$ ) many unknown peaks are observed in the PXD pattern. At about  $70\text{ }^\circ\text{C}$ , an exothermic peak is observed in the HP-DSC trace (**Figure 5, C**) possibly due a further formation of the unknown phase



or to the transition of the  $\gamma$ -Mg(BH<sub>4</sub>)<sub>2</sub> phase. At T<sub>peak</sub>= 114 °C (approx. 102 °C on cooling) the PT of LiBH<sub>4</sub> has been observed, followed by an endothermic signal at T<sub>peak</sub>= 126 °C, which is present only on the first cycle. This thermal event could be related to a phase transformation that turns out irreversible on cooling, so that it is not observed in the second heating ramp. At T<sub>peak</sub>= 145 °C (approx. 115 °C on cooling) and T<sub>peak</sub>= 153 °C (approx. 137 °C on cooling), some melting (solidification) reactions are occurring and a liquidus temperature is observed at 173 °C. The LiMgCa system releases hydrogen at T<sub>peak</sub>= 374 °C, 382 °C and 393 °C (**Figure 5, D**).

#### *NaBH<sub>4</sub>-KBH<sub>4</sub>-Mg(BH<sub>4</sub>)<sub>2</sub>*

Considering ternary mixtures without LiBH<sub>4</sub>, in the NaKMg system (**Figure 6, A**), only NaBH<sub>4</sub> and KBH<sub>4</sub> are observed in the PXD pattern after BM (**Figure 6, B, BM**), signal from Mg(BH<sub>4</sub>)<sub>2</sub> are hardly visible because of its low scattering and low crystallinity due to ball milling.[11] After annealing, the formation of the cubic NaBH<sub>4</sub>-KBH<sub>4</sub> solid solution is occurring, as evidenced from shoulders in the PXD peaks of pristine phases (**Figure 6, B, 200 °C**). The HP-DSC trace presents only an exothermic peak around 90 °C on the first cycle (**Figure 6, C**) that can be related to the formation of the equilibrium phases mixture. The NaKMg system releases a small amount of hydrogen above 200 °C in a large temperature range, but no clear DTA signals are recorded (**Figure 6, D**). This behaviour is similar to that of pure Mg(BH<sub>4</sub>)<sub>2</sub>. [11],[46],[47]

#### *NaBH<sub>4</sub>-KBH<sub>4</sub>-Ca(BH<sub>4</sub>)<sub>2</sub>*

In the NaKCa system (**Figure 7, A**), the formation of the bimetallic KCa(BH<sub>4</sub>)<sub>3</sub> compound is observed again after BM, together with residual NaBH<sub>4</sub>, KBH<sub>4</sub> and  $\alpha$ -Ca(BH<sub>4</sub>)<sub>2</sub> phases (**Figure 7, B, BM**). After annealing, the intensity of PXD peaks of the KCa(BH<sub>4</sub>)<sub>3</sub> phase increases, while those related to NaBH<sub>4</sub> and KBH<sub>4</sub> decrease and the  $\alpha$ -Ca(BH<sub>4</sub>)<sub>2</sub> phase disappears (**Figure 7, B, 200 °C**). In the HP-DSC trace, only the PT of KCa(BH<sub>4</sub>)<sub>3</sub> can be identified at T<sub>peak</sub>= 72 °C (61 °C on cooling), which becomes more intense on the second cycle (**Figure 7, C**). In the NaKCa system, the decomposition temperature of KCa(BH<sub>4</sub>)<sub>3</sub> is lowered by the addition of NaBH<sub>4</sub> to T<sub>peak</sub>= 311 °C and further decomposition occurs at T<sub>peak</sub>= 382 °C and 439 °C (**Figure 7, D**).

### *NaBH<sub>4</sub>-Mg(BH<sub>4</sub>)<sub>2</sub>-Ca(BH<sub>4</sub>)<sub>2</sub>*

The NaMgCa system (**Figure 8, A**) presents NaBH<sub>4</sub>,  $\gamma$ -Mg(BH<sub>4</sub>)<sub>2</sub> and  $\alpha$ -Ca(BH<sub>4</sub>)<sub>2</sub> phases after ball milling (**Figure 8, B, BM**). After annealing, NaBH<sub>4</sub>,  $\gamma$ -Mg(BH<sub>4</sub>)<sub>2</sub> and  $\alpha$ -Ca(BH<sub>4</sub>)<sub>2</sub> phases are still present (**Figure 8, B, 200 °C**). In addition, unknown PXD peaks can be observed, similar to those observed for the LiMgCa sample. The HP-DSC trace presents many broad peaks, with low intensity on heating possibly related to some reactions of the unknown phase. On the other hand they can be assigned to partial melting or to the PT of Ca(BH<sub>4</sub>)<sub>2</sub> and Mg(BH<sub>4</sub>)<sub>2</sub> around 160 °C (**Figure 8, C**). In the NaMgCa system, hydrogen release occurs in three main events at  $T_{\text{peak}} = 261$  °C, 369 °C and 436 °C (**Figure 8, D**).

### *KBH<sub>4</sub>-Mg(BH<sub>4</sub>)<sub>2</sub>-Ca(BH<sub>4</sub>)<sub>2</sub>*

In the KMgCa system (**Figure 9, A**), KBH<sub>4</sub>,  $\alpha$ -Ca(BH<sub>4</sub>)<sub>2</sub> and KCa(BH<sub>4</sub>)<sub>3</sub> phases are present after ball milling (**Figure 9, B, BM**), but PXD peaks from Mg(BH<sub>4</sub>)<sub>2</sub> are hardly observed because of low scattering. After annealing, PXD peaks of KCa(BH<sub>4</sub>)<sub>3</sub> compound slightly increase, while PXD peaks KBH<sub>4</sub> decrease and traces of PXD peaks of  $\beta$ -Ca(BH<sub>4</sub>)<sub>2</sub> can be observed (**Figure 9, B, 200 °C**). As for the NaKCa system, in the HP-DSC trace, only the PT of KCa(BH<sub>4</sub>)<sub>3</sub> can be identified at  $T_{\text{peak}} = 72$  °C (62 °C on cooling), which becomes slightly more intense on the second cycle (**Figure 9, C**). Hydrogen release occurs at  $T_{\text{peak}} = 383$  °C, as for KCa(BH<sub>4</sub>)<sub>3</sub> (**Figure 9, D**).

## **Quaternary systems**

### *LiBH<sub>4</sub>-NaBH<sub>4</sub>-KBH<sub>4</sub>-Mg(BH<sub>4</sub>)<sub>2</sub>*

For the LiNaKMg system (**Figure 10, A**), after BM, the formation of LiKMg(BH<sub>4</sub>)<sub>4</sub> and LiK(BH<sub>4</sub>)<sub>2</sub> is observed, together with the presence of LiBH<sub>4</sub>, NaBH<sub>4</sub>, KBH<sub>4</sub>,  $\gamma$ -Mg(BH<sub>4</sub>)<sub>2</sub> and  $\alpha$ -Mg(BH<sub>4</sub>)<sub>2</sub> (**Figure 10, B, BM**). The Li<sub>2</sub>K<sub>3</sub>Mg<sub>2</sub>(BH<sub>4</sub>)<sub>9</sub> compound is observed after annealing in the PXD pattern, together with LiKMg(BH<sub>4</sub>)<sub>4</sub>, NaBH<sub>4</sub>,  $\alpha$ -Mg(BH<sub>4</sub>)<sub>2</sub>,  $\beta$ -Mg(BH<sub>4</sub>)<sub>2</sub> and small amount of KBH<sub>4</sub> (**Figure 10, B, 200 °C**). The HP-DSC trace is similar to that obtained for the LiKMg system, where three main events can be observed on heating in the temperature range from 80 to 110 °C,

consisting in the PT of  $\text{LiBH}_4$ , the reaction to form  $\text{Li}_2\text{K}_3\text{Mg}_2(\text{BH}_4)_9$  and the melting of the  $\text{LiBH}_4$ - $\text{KBH}_4$  eutectic (**Figure 10, C**). [26],[49] Only on the first cooling ramp the reaction of the trimetallic compound is observed at  $T_{\text{peak}} = 67\text{ }^\circ\text{C}$ , which explains the residual  $\text{Li}_2\text{K}_3\text{Mg}_2(\text{BH}_4)_9$  observed in PXD after thermal treatment. The  $\text{LiNaKMg}$  system releases hydrogen at  $T_{\text{peak}} = 320\text{ }^\circ\text{C}$ ,  $394\text{ }^\circ\text{C}$  and  $484\text{ }^\circ\text{C}$  (**Figure 10, D**), similarly to what observed for the  $\text{LiKMg}$  system.

#### ***$\text{LiBH}_4\text{-NaBH}_4\text{-KBH}_4\text{-Ca}(\text{BH}_4)_2$***

In the  $\text{LiNaKCa}$  system (**Figure 11, A**), the milled mixture presents  $\text{LiBH}_4$ ,  $\text{NaBH}_4$ ,  $\text{KBH}_4$ ,  $\alpha\text{-Ca}(\text{BH}_4)_2$  and  $\text{KCa}(\text{BH}_4)_3$  phases (**Figure 11, B, BM**). The phase mixture does not change after annealing, except for  $\alpha\text{-Ca}(\text{BH}_4)_2$  that disappears (**Figure 11, B, 200 °C**). The HP-DSC trace shows the PT of  $\text{KCa}(\text{BH}_4)_3$  at  $T_{\text{peak}} = 73\text{ }^\circ\text{C}$  ( $66\text{ }^\circ\text{C}$  on cooling), the melting of  $\text{LiNaK}$  or  $\text{LiNaCa}$  ternary eutectic at  $T_{\text{peak}} = 99\text{ }^\circ\text{C}$  ( $90\text{ }^\circ\text{C}$  on cooling) and the liquidus temperature at  $156\text{ }^\circ\text{C}$  ( $142\text{ }^\circ\text{C}$  on cooling) (**Figure 11, C**). For the first time, a liquid phase containing four different borohydrides is clearly observed. The  $\text{LiNaKCa}$  system releases hydrogen at  $T_{\text{peak}} = 295\text{ }^\circ\text{C}$  and above  $350\text{ }^\circ\text{C}$  (**Figure 11, D**). It is worth noting that the addition of  $\text{LiBH}_4$  to the  $\text{NaKCa}$  sample reduces the hydrogen release temperatures.

#### ***$\text{LiBH}_4\text{-NaBH}_4\text{-Mg}(\text{BH}_4)_2\text{-Ca}(\text{BH}_4)_2$***

The  $\text{LiNaMgCa}$  system (**Figure 12, A**) presents  $\text{LiBH}_4$ ,  $\text{NaBH}_4$ ,  $\gamma\text{-Mg}(\text{BH}_4)_2$ ,  $\alpha\text{-Mg}(\text{BH}_4)_2$  and  $\alpha\text{-Ca}(\text{BH}_4)_2$  phases after ball milling (**Figure 12, B, BM**). After annealing, only  $\text{NaBH}_4$  and  $\alpha\text{-Ca}(\text{BH}_4)_2$  phases are still clearly visible, together with some PXD halos, that may be related to reactions of  $\text{Mg}(\text{BH}_4)_2$  due to thermal treatment (**Figure 12, B, 200 °C**). [46],[47] The thermal events observed in the HP-DSC trace (**Figure 12, C**) suggest the occurrence of multiple melting reactions, mainly occurring at  $T_{\text{peak}} = 96\text{ }^\circ\text{C}$  and  $99\text{ }^\circ\text{C}$  ( $85\text{ }^\circ\text{C}$  on cooling). The liquidus temperature is recorded at  $156\text{ }^\circ\text{C}$  ( $99\text{ }^\circ\text{C}$  on cooling), underlining again that a quaternary liquid phase is formed. The  $\text{LiNaMgCa}$  system releases hydrogen at  $T_{\text{peak}} = 280\text{ }^\circ\text{C}$ ,  $369\text{ }^\circ\text{C}$  and  $468\text{ }^\circ\text{C}$  (**Figure 12, D**).

#### ***$\text{LiBH}_4\text{-KBH}_4\text{-Mg}(\text{BH}_4)_2\text{-Ca}(\text{BH}_4)_2$***

After milling, the LiKMgCa system (**Figure 13, A**) is characterized by the formation of  $\text{KCa}(\text{BH}_4)_3$  compound and by the presence of  $\text{LiBH}_4$ ,  $\text{KBH}_4$ , and  $\alpha\text{-Mg}(\text{BH}_4)_2$  phases (**Figure 13, B, BM**). After annealing, only traces of  $\text{LiBH}_4$  are present, together with some PXD peaks at low angles, that indicate the formation of a small quantity of  $\text{LiKMg}(\text{BH}_4)_4$  (**Figure 13, B, 200 °C**). **Figure 13, C** shows the HP-DSC trace of the LiKMgCa mixture. It is characterized by the PT of  $\text{KCa}(\text{BH}_4)_3$  at  $T_{\text{peak}} = 75\text{ °C}$  ( $65\text{ °C}$  on cooling), the PT of  $\text{LiBH}_4$  at  $T_{\text{peak}} = 113\text{ °C}$  ( $104\text{ °C}$  on cooling), the melting of a ternary eutectic at  $T_{\text{peak}} = 126\text{ °C}$  ( $112\text{ °C}$  on cooling), that could be related to the LiMgCa system, and a liquidus temperature at  $157\text{ °C}$  ( $137\text{ °C}$  on cooling). On cooling, the double peak at low temperatures indicates the reaction of  $\text{LiKMg}(\text{BH}_4)_4$  at  $T_{\text{peak}} = 67\text{ °C}$ . [26],[49] The LiKMgCa system releases hydrogen at  $T_{\text{peak}} = 319\text{ °C}$ ,  $370\text{ °C}$  and  $444\text{ °C}$  (**Figure 13, D**).

#### ***NaBH<sub>4</sub>-KBH<sub>4</sub>-Mg(BH<sub>4</sub>)<sub>2</sub>-Ca(BH<sub>4</sub>)<sub>2</sub>***

After ball milling, the NaKMgCa system (**Figure 14, A**) shows the presence of  $\text{NaBH}_4$ ,  $\text{KBH}_4$ ,  $\alpha\text{-Mg}(\text{BH}_4)_2$ ,  $\alpha\text{-Ca}(\text{BH}_4)_2$  and  $\text{KCa}(\text{BH}_4)_3$  phases (**Figure 14, B, BM**). After annealing, only  $\text{NaBH}_4$  and  $\text{KCa}(\text{BH}_4)_3$  are clearly observed. Also in this case, the presence of halos in the PXD pattern indicates the possible reaction of  $\text{Mg}(\text{BH}_4)_2$  upon thermal treatment (**Figure 14, B, 200 °C**). [46],[47] In the HP-DSC trace, only the PT of  $\text{KCa}(\text{BH}_4)_3$  can be detected at  $T_{\text{peak}} = 75\text{ °C}$ , while the peak at  $T_{\text{peak}} = 166\text{ °C}$  ( $129\text{ °C}$  on cooling) is related to a melting reaction with a strong undercooling (**Figure 14, C**). The NaKMgCa system releases hydrogen at  $T_{\text{peak}} = 293\text{ °C}$ ,  $367\text{ °C}$  and  $477\text{ °C}$  (**Figure 14, D**).

## **Discussions and conclusions**

The explorative investigation of many ternary and quaternary combinations of borohydrides in the  $\text{LiBH}_4\text{-NaBH}_4\text{-KBH}_4\text{-Mg}(\text{BH}_4)_2\text{-Ca}(\text{BH}_4)_2$  system has evidenced some common features in various systems.

In the as milled samples, as a general observation, no appreciable interactions to form solid solutions have been observed. Actually, the formation of bi/tri-metallic compounds is observed.

KCa(BH<sub>4</sub>)<sub>3</sub> compound is always formed when KBH<sub>4</sub> and Ca(BH<sub>4</sub>)<sub>2</sub> borohydrides are present in the mixture, i.e. LiKCa, NaKCa, KMgCa, LiNaKCa, LiKMgCa and NaKMgCa systems. Its enthalpy of formation is likely strongly negative, limiting overcoming possible entropy contributions to the free energy of solid solutions based on multiple borohydrides.

When Mg(BH<sub>4</sub>)<sub>2</sub> is present in mixture with LiBH<sub>4</sub> and KBH<sub>4</sub>, i.e. LiKMg, LiNaKMg and LiKMgCa systems, the trimetallic LiKMg(BH<sub>4</sub>)<sub>4</sub> compound can be formed, often together with the presence of an excess of LiK(BH<sub>4</sub>)<sub>2</sub>. On the other hand, LiK(BH<sub>4</sub>)<sub>2</sub> is not formed when Ca(BH<sub>4</sub>)<sub>2</sub> is present in the mixture (LiKMgCa system), because of the high stability of the bimetallic KCa(BH<sub>4</sub>)<sub>3</sub> compound, due to its strongly negative free energy of formation, that likely overcome that of any other phase involving KBH<sub>4</sub>.

No K<sub>2</sub>Mg(BH<sub>4</sub>)<sub>4</sub> or K<sub>3</sub>Mg(BH<sub>4</sub>)<sub>5</sub> compounds are observed to form in mixture where both KBH<sub>4</sub> and Mg(BH<sub>4</sub>)<sub>2</sub> are present,[23] likely due to a lower thermodynamic stability with respect to that of above reported bi/trimetallic compounds. Furthermore, in the NaKMg system, these compounds are not formed either, since the interaction between NaBH<sub>4</sub> and KBH<sub>4</sub> favoured the formation of the Na<sub>x</sub>K<sub>(1-x)</sub>BH<sub>4</sub> solid solution.

When both Mg(BH<sub>4</sub>)<sub>2</sub> and Ca(BH<sub>4</sub>)<sub>2</sub> are present in the mixture, several unidentified PXD peaks are observed, likely related to an unknown compound (LiMgCa and NaMgCa). However, its formation is hindered when KBH<sub>4</sub> is also present, because it is reacting with Ca(BH<sub>4</sub>)<sub>2</sub>, to form the bimetallic KCa(BH<sub>4</sub>)<sub>3</sub>. The only exception is the LiNaMgCa system, where the unknown compound potentially involving Mg(BH<sub>4</sub>)<sub>2</sub> and Ca(BH<sub>4</sub>)<sub>2</sub> is not formed. The unknown phase could contain only Mg(BH<sub>4</sub>)<sub>2</sub> and Ca(BH<sub>4</sub>)<sub>2</sub>, however its exact composition has not been determined yet. In an ongoing study,[25] the Mg(BH<sub>4</sub>)<sub>2</sub>-Ca(BH<sub>4</sub>)<sub>2</sub> system is systematically investigated in order to define the composition, thermal stability and possible role of Mg(BH<sub>4</sub>)<sub>2</sub> polymorphs in the formation of the unknown phase.

A limited formation of solid solutions can be observed only after thermal treatment. The Na<sub>x</sub>K<sub>(1-x)</sub>BH<sub>4</sub> solid solution is clearly formed in the NaKMg system. On the other hand, in other systems,

the high driving force for the formation of bi/tri-metallic compounds involving  $\text{KBH}_4$  hindered the formation of the  $\text{Na}_x\text{K}_{(1-x)}\text{BH}_4$  cubic solid solution.

No values of enthalpies of formation are reported in the literature for observed bi/tri-metallic compounds. Nevertheless, an estimation of the relative stabilities of these compounds can be evidenced from the results of the present study.  $\text{KCa}(\text{BH}_4)_3$  has likely the lowest free energy, since its formation is strongly favoured, followed by  $\text{LiKMg}(\text{BH}_4)_4$  and then  $\text{LiK}(\text{BH}_4)_2$ . The binary  $\text{LiK}(\text{BH}_4)_2$  compound was reported to be unstable at 300 K by Kim et al.[50]. For the reaction between  $\text{LiBH}_4$  and  $\text{KBH}_4$  to form  $\text{LiK}(\text{BH}_4)_2$ , the calculated Gibbs free energy at 300 K was reported to be positive, with an enthalpy of reaction  $\Delta H_{300\text{K}} = -1300 \text{ J/mol}$ . Nevertheless, this compound is usually formed upon grinding  $\text{LiBH}_4$  and  $\text{KBH}_4$ , being stable up to  $96 \text{ }^\circ\text{C}$ , as reported by Ley et al.[13]. The present study confirms the formation of this phase in equimolar mixtures of  $\text{LiBH}_4$  and  $\text{KBH}_4$ , suggesting the occurrence of a negative Gibbs free energy for the reaction at 300 K, as reported by Dematteis et al.[6].

The enthalpy of mixing for the equimolar  $\text{Na}_x\text{K}_{(1-x)}\text{BH}_4$  solid solution, which is positive (i.e. equal to  $1973 \text{ J/mol}$ [6]), underlining the lower tendency for the solid solution to be formed.

Regarding the liquid phase, the investigation of equimolar ternary and quaternary combinations in the  $\text{LiBH}_4\text{-NaBH}_4\text{-KBH}_4\text{-Mg}(\text{BH}_4)_2\text{-Ca}(\text{BH}_4)_2$  system evidenced the presence of possible new ternary eutectics, such as in the  $\text{LiNaMg}$ ,  $\text{LiKCa}$ ,  $\text{LiMgCa}$ ,  $\text{LiNaMgCa}$  and  $\text{LiKMgCa}$  mixtures. Such new ternary eutectics have a melting temperature in the range from  $100 \text{ }^\circ\text{C}$  to  $140 \text{ }^\circ\text{C}$ , a temperature range much lower than that observed for binary eutectics involving  $\text{LiBH}_4$ ,  $\text{NaBH}_4$ ,  $\text{Mg}(\text{BH}_4)_2$  and  $\text{Ca}(\text{BH}_4)_2$ . Also the  $\text{KCa}(\text{BH}_4)_3$  is involved in these eutectic reactions. Partial melting can be involved at high temperatures for the  $\text{NaKCa}$  and  $\text{NaKMgCa}$  systems as previously observed in the  $\text{NaCa}$  and  $\text{NaMg}$  systems.[22]

The hydrogen desorption in ternary and quaternary equimolar mixtures usually occurs from the liquid phase, via a complex multi-steps reactions. The presence of  $\text{LiBH}_4$  generally promotes the release of  $\text{H}_2$  at low temperatures ( $\text{LiNaMg}$ ,  $\text{LiNaKCa}$  and  $\text{LiNaMgCa}$ ).  $\text{KCa}(\text{BH}_4)_3$  promotes the

release in a single-step reaction, but at higher temperatures (LiKCa, NaKCa, KMgCa, LiKMgCa and NaKMgCa). Partial decomposition is also observed in the LiNaMg, LiNaMgCa and LiKMgCa systems, where a halo is observed in the PXD pattern after thermal treatment up to 200°C, which can be related to the formation of boron-based compounds, because of reactions or decomposition of  $\text{Mg}(\text{BH}_4)_2$ . [46],[47] However, no significant differences or only slight improvement in the main hydrogen release temperatures are observed, comparing the investigated systems with the quinary equimolar mixture previously investigated by the present authors. [11]

Following the concept of High Entropy Phases, [51] it is expected that, in a multicomponent system, a solid solution could be stabilized because of the high entropy of configuration. In the case of cation substitution in borohydrides, the increase of configurational entropy, due to an increase of constituents in the mixture, takes advantage from one sublattice only. On the other hand, the substitution in a cation sublattice with more electronegative elements is expected to promote the release of hydrogen at lower temperature, because of a stronger interaction with the  $\text{BH}_4^-$  anion, which reduce the energy of the B-H bond and improve hydrogen release.

From a general overview of reported results, as previously discussed by Dematteis et al., [11] it is evident that the combination of different borohydrides up to quaternary mixtures did not bring to the formation of a single-phase solid solution. In fact, the substitutions in the cationic sublattice in the solid phases are limited and strictly connected to original crystal structures, cation coordination and stability of intermetallic compounds. While solid phases are immiscible, miscibility in the liquid phase have been evidenced, [2] leading to hydrogen release from the liquid phase.

To conclude, on the basis of these explorative analysis, a new phase is formed in the LiMgCa and NaMgCa system, due to a possible interaction between  $\text{Mg}(\text{BH}_4)_2$  and  $\text{Ca}(\text{BH}_4)_2$ . The results from this study are expected to be a solid base for a further optimisation and assessment of thermodynamic properties of borohydrides in complex mixtures and systems, which will enable the development of a complete database for thermodynamic calculations and predictions of melting

reactions, solid solutions, compounds formation and hydrogen release reactions as a function of temperature and composition.

## Acknowledgement

Financial support from the ITN Marie Curie ECOSTORE (Grant agreement n° 607040) is thankfully acknowledged. EMD acknowledges the Erasmus Traineeship Programme for the financial support in the exchange mobility period between the HZG and the University of Turin.

## References

- [1] Paskevicius, M. , Jepsen, L. H. , Schouwink, P. , Černý, R. , Ravnsbæk, D. B. , Filinchuk, Y. , Dornheim, M. , Besenbacher, F. , and Jensen, T. R. Metal borohydrides and derivatives – synthesis, structure and properties. *Chemical Society Reviews* **2017**, 46, 1565–1634.
- [2] Milanese, C. , Jensen, T. . , Hauback, B. C. , Pistidda, C. , Dornheim, M. , Yang, H. , Lombardo, L. , Züttel, A. , Filinchuk, Y. , Ngene, P. , Jongh, P. E. de , Buckley, C. E. , Dematteis, E. M. , and Baricco, M. Complex hydrides for energy storage. *International Journal of Hydrogen Energy* **2018**, Accepted
- [3] Kharbachi, A. El , Pinatel, E. R. , Nutta, I. , and Baricco, M. A thermodynamic assessment of LiBH<sub>4</sub>. *Calphad* **2012**, 39, 80–90.
- [4] Orimo, S. I. , Nakamori, Y. , Kitahara, G. , Miwa, K. , Ohba, N. , Towata, S. , and Züttel, A. Dehydrogenating and rehydrogenating reactions of LiBH<sub>4</sub>. *Journal of Alloys and Compounds* **2005**, 404–406, 427–430.
- [5] Milanese, C. , Garroni, S. , Girella, A. , Mulas, G. , Berbenni, V. , Bruni, G. , Suriñach, S. , Baró, M. D. , and Marini, A. Thermodynamic and Kinetic Investigations on Pure and Doped NaBH<sub>4</sub>–MgH<sub>2</sub> System. *The Journal of Physical Chemistry C* **2011**, 115, 3151–3162.
- [6] Dematteis, E. M. , Pinatel, E. R. , Corno, M. , Jensen, T. R. , and Baricco, M. Phase diagrams of the LiBH<sub>4</sub>–NaBH<sub>4</sub>–KBH<sub>4</sub> system. *Physical Chemistry Chemical Physics* **2017**, 19, 25071–25079.
- [7] Stasinevich, D. S. and Egorenko, G. A. Thermographic Investigation of Alkali Metal and Magnesium Tetrahydroborates at pressures up to 10 atm. *Russian Journal of Inorganic Chemistry* **1968**, 13, 341–343.
- [8] Pinatel, E. R. , Albanese, E. , Civalleri, B. , and Baricco, M. Thermodynamic modelling of Mg(BH<sub>4</sub>)<sub>2</sub>. *Journal of Alloys and Compounds* **2015**, 645, S64–S68.
- [9] Borgschulte, A. , Gremaud, R. , Züttel, A. , Martelli, P. , Remhof, A. , Ramirez-Cuesta, A. J. , Refson, K. , Bardaji, E. G. , Lohstroh, W. , Fichtner, M. , Hagemann, H. , and Ernst, M. Experimental evidence of librational vibrations determining the stability of calcium borohydride. *Physical Review B* **2011**, 83, 024102.
- [10] Mao, J. , Guo, Z. , Poh, C. K. , Ranjbar, A. , Guo, Y. , Yu, X. , and Liu, H. Study on the dehydrogenation kinetics and thermodynamics of Ca(BH<sub>4</sub>)<sub>2</sub>. *Journal of Alloys and Compounds* **2010**, 500, 200–205.
- [11] Dematteis, E. M. , Santoru, A. , Poletti, M. G. , Pistidda, C. , Klassen, T. , Dornheim, M. , and Baricco, M. Phase stability and hydrogen desorption in a quinary equimolar mixture of light-metals borohydrides. *International Journal of Hydrogen Energy* **2018**, 43, 16793–16803.
- [12] Roedern, E. , Hansen, B. R. S. , Ley, M. B. , and Jensen, T. R. Effect of Eutectic Melting, Reactive Hydride Composites, and Nanoconfinement on Decomposition and Reversibility of LiBH<sub>4</sub>–KBH<sub>4</sub>. *The Journal of Physical Chemistry C* **2015**, 119, 25818–25825.
- [13] Ley, M. B. , Roedern, E. , and Jensen, T. R. Eutectic melting of LiBH<sub>4</sub>–KBH<sub>4</sub>. *Phys. Chem. Chem. Phys.* **2014**, 16, 24194–24199.
- [14] Dematteis, E. M. , Roedern, E. , Pinatel, E. R. , Corno, M. , Jensen, T. R. , and Baricco, M. A thermodynamic investigation of the LiBH<sub>4</sub>–NaBH<sub>4</sub> system. *RSC Advances* **2016**, 6, 60101–60108.
- [15] Liu, Y. , Reed, D. , Paterakis, C. , Contreras Vasquez, L. , Baricco, M. , and Book, D. Study of the decomposition of a 0.62LiBH<sub>4</sub>–0.38NaBH<sub>4</sub> mixture. *International Journal of Hydrogen Energy* **2017**, 42, 22480–22488.
- [16] Liu, X. , Peaslee, D. , Sheehan, T. P. , and Majzoub, E. H. Decomposition Behavior of Eutectic LiBH<sub>4</sub>–Mg(BH<sub>4</sub>)<sub>2</sub> and Its Confinement Effects in Ordered Nanoporous Carbon. *The Journal of Physical Chemistry C* **2014**, 118, 27265–27271.
- [17] Fang, Z.-Z. , Kang, X.-D. , Wang, P. , Li, H.-W. , and Orimo, S.-I. Unexpected dehydrogenation behavior of LiBH<sub>4</sub>/Mg(BH<sub>4</sub>)<sub>2</sub> mixture associated with the in situ formation of dual-cation borohydride. *Journal of Alloys and Compounds* **2010**, 491, L1–L4.
- [18] Bardají, E. G. , Zhao-Karger, Z. , Boucharat, N. , Nale, A. , Setten, M. J. van , Lohstroh, W. , Röhm, E. , Catti, M. ,



- and Fichtner, M.  $\text{LiBH}_4\text{-Mg}(\text{BH}_4)_2$ : A Physical Mixture of Metal Borohydrides as Hydrogen Storage Material. *The Journal of Physical Chemistry C* **2011**, 115, 6095–6101.
- [19] Lee, J. Y. , Ravnsbæk, D. B. , Lee, Y. S. , Kim, Y. , Cerenius, Y. , Shim, J. , Jensen, T. R. , Hur, N. H. , and Cho, Y. W. Decomposition Reactions and Reversibility of the  $\text{LiBH}_4\text{-Ca}(\text{BH}_4)_2$  Composite. *The Journal of Physical Chemistry C* **2009**, 113, 15080–15086.
- [20] Lee, H. S. , Lee, Y. S. , Suh, J. Y. , Kim, M. , Yu, J. S. , and Cho, Y. W. Enhanced Desorption and Absorption Properties of Eutectic  $\text{LiBH}_4\text{-Ca}(\text{BH}_4)_2$  Infiltrated into Mesoporous Carbon. *The Journal of Physical Chemistry C* **2011**, 115, 20027–20035.
- [21] Jensen, S. R. H. , Jepsen, L. H. , Skibsted, J. , and Jensen, T. R. Phase Diagram for the  $\text{NaBH}_4\text{-KBH}_4$  System and the Stability of a  $\text{Na}(1-x)\text{K}(x)\text{BH}_4$  Solid Solution. *The Journal of Physical Chemistry C* **2015**, 119, 27919–27929.
- [22] Ley, M. B. , Roedern, E. , Thygesen, P. , and Jensen, T. R. Melting Behavior and Thermolysis of  $\text{NaBH}_4\text{-Mg}(\text{BH}_4)_2$  and  $\text{NaBH}_4\text{-Ca}(\text{BH}_4)_2$  Composites. *Energies* **2015**, 8, 2701–2713.
- [23] Schouwink, P. , D'Anna, V. , Ley, M. B. , Lawson Daku, L. M. , Richter, B. , Jensen, T. R. , Hagemann, H. , and Černý, R. Bimetallic Borohydrides in the System  $\text{M}(\text{BH}_4)_2\text{-KBH}_4$  ( $\text{M} = \text{Mg}, \text{Mn}$ ): On the Structural Diversity. *The Journal of Physical Chemistry C* **2012**, 116, 10829–10840.
- [24] Schouwink, P. , Ley, M. B. , Tissot, A. , Hagemann, H. , Jensen, T. R. , Smrčok, L. , and Černý, R. Structure and properties of complex hydride perovskite materials. *Nature Communications* **2014**, 5706, 1–10.
- [25] Dematteis, E. M. , Sturari, S. , Pistidda, C. , and Baricco, M. Phase Diagram for the  $\text{Mg}(\text{BH}_4)_2\text{-Ca}(\text{BH}_4)_2$  System. *to be submitted*
- [26] Černý, R. , Schouwink, P. , Sadikin, Y. , Stare, K. , Smrčok, L. , Richter, B. , and Jensen, T. R. Trimetallic Borohydride  $\text{Li}_3\text{M}_2\text{Zn}_5(\text{BH}_4)_{15}$  ( $\text{M} = \text{Mg}, \text{Mn}$ ) Containing Two Weakly Interconnected Frameworks. *Inorganic Chemistry* **2013**, 52, 9941–9947.
- [27] Schouwink, P. , Ramel, A. , Giannini, E. , and Černý, R. Flux-assisted single crystal growth and heteroepitaxy of perovskite-type mixed-metal borohydrides. *CrystEngComm* **2015**, 17, 2682–2689.
- [28] Vajo, J. J. Influence of nano-confinement on the thermodynamics and dehydrogenation kinetics of metal hydrides. *Current Opinion in Solid State and Materials Science* **2011**, 15, 52–61.
- [29] Jongh, P. E. De , Allendorf, M. , Vajo, J. J. , and Zlotea, C. Nanoconfined light metal hydrides for reversible hydrogen storage. *MRS Bulletin* **2013**, 38, 488–494.
- [30] Rude, L. H. , Nielsen, T. K. , Ravnsbæk, D. B. , Bösenberg, U. , Ley, M. B. , Richter, B. , Arnbjerg, L. M. , Dornheim, M. , Filinchuk, Y. , Besenbacher, F. , and Jensen, T. R. Tailoring properties of borohydrides for hydrogen storage: A review. *physica status solidi (a)* **2011**, 208, 1754–1773.
- [31] Puszkiel, J. , Garroni, S. , Milanese, C. , Gennari, F. , Klassen, T. , Dornheim, M. , and Pistidda, C. Tetrahydroborates: Development and Potential as Hydrogen Storage Medium. *Inorganics* **2017**, 5, 74.
- [32] Dematteis, E. M. , Vaunois, S. , Pistidda, C. , Dornheim, M. , and Baricco, M. Reactive Hydride Composite of  $\text{Mg}_2\text{NiH}_4$  with Borohydrides Eutectic Mixtures. *Crystals* **2018**, 8, 90.
- [33] Bergemann, N. , Pistidda, C. , Milanese, C. , Emmeler, T. , Karimi, F. , Chaudhary, A.-L. , Chierotti, M. R. , Klassen, T. , and Dornheim, M.  $\text{Ca}(\text{BH}_4)_2\text{-Mg}_2\text{NiH}_4$ : on the pathway to a  $\text{Ca}(\text{BH}_4)_2$  system with a reversible hydrogen cycle. *Chem. Commun.* **2016**, 52, 4836–4839.
- [34] Hu, J. , Fichtner, M. , and Baricco, M. Preparation of  $\text{Li-Mg-N-H}$  hydrogen storage materials for an auxiliary power unit. *International Journal of Hydrogen Energy* **2017**, 42, 17144–17148.
- [35] Pistidda, C. , Napolitano, E. , Pottmaier, D. , Dornheim, M. , Klassen, T. , Baricco, M. , and Enzo, S. Structural study of a new B-rich phase obtained by partial hydrogenation of  $2\text{NaH} + \text{MgB}_2$ . *International Journal of Hydrogen Energy* **2013**, 38, 10479–10484.
- [36] Pistidda, C. , Pottmaier, D. , Karimi, F. , Garroni, S. , Rzeszutek, A. , Tolkiehn, M. , Fichtner, M. , Lohstroh, W. , Baricco, M. , Klassen, T. , and Dornheim, M. Effect of  $\text{NaH/MgB}_2$  ratio on the hydrogen absorption kinetics of the system  $\text{NaH} + \text{MgB}_2$ . *International Journal of Hydrogen Energy* **2014**, 39, 5030–5036.
- [37] Garroni, S. , Minella, C. B. , Pottmaier, D. , Pistidda, C. , Milanese, C. , Marini, A. , Enzo, S. , Mulas, G. , Dornheim, M. , Baricco, M. , Gutfleisch, O. , Suriñach, S. , and Baró, M. D. Mechanochemical synthesis of  $\text{NaBH}_4$  starting from  $\text{NaH-MgB}_2$  reactive hydride composite system. *International Journal of Hydrogen Energy* **2013**, 38, 2363–2369.
- [38] Paskevicius, M. , Ley, M. B. , Sheppard, D. A. , Jensen, T. R. , and Buckley, C. E. Eutectic melting in metal borohydrides. *Physical Chemistry Chemical Physics* **2013**, 15, 19774.
- [39] Javadian, P. , Sheppard, D. A. , Buckley, C. E. , and Jensen, T. R. Hydrogen storage properties of nanoconfined  $\text{LiBH}_4\text{-NaBH}_4$ . *International Journal of Hydrogen Energy* **2015**, 40, 14916–14924.
- [40] Zhao-Karger, Z. , Witter, R. , Bardaji, E. G. , Wang, D. , Cossement, D. , and Fichtner, M. Altered reaction pathways of eutectic  $\text{LiBH}_4\text{-Mg}(\text{BH}_4)_2$  by nanoconfinement. *Journal of Materials Chemistry A* **2013**, 1, 3379.
- [41] Javadian, P. and Jensen, T. R. Enhanced hydrogen reversibility of nanoconfined  $\text{LiBH}_4\text{-Mg}(\text{BH}_4)_2$ . *International Journal of Hydrogen Energy* **2014**, 39, 9871–9876.
- [42] Lee, Y.-S. , Filinchuk, Y. , Lee, H. S. , Suh, J.-Y. , Kim, J. W. , Yu, J.-S. , and Cho, Y. W. On the Formation and the Structure of the First Bimetallic Borohydride Borate,  $\text{LiCa}_3(\text{BH}_4)(\text{BO}_3)_2$ . *The Journal of Physical Chemistry C* **2011**, 115, 10298–10304.

- [43] Ampoumogli, A. , Charalambopoulou, G. , Javadian, P. , Richter, B. , Jensen, T. R. , and Steriotis, T. Hydrogen desorption and cycling properties of composites based on mesoporous carbons and a LiBH<sub>4</sub>-Ca(BH<sub>4</sub>)<sub>2</sub> eutectic mixture. *Journal of Alloys and Compounds* **2015**, 645, S480-S484.
- [44] Javadian, P. , Sheppard, D. A. , Buckley, C. E. , and Jensen, T. R. Hydrogen storage properties of nanoconfined LiBH<sub>4</sub>-Ca(BH<sub>4</sub>)<sub>2</sub>. *International Journal of Hydrogen Energy* **2015**, 11, 96-103.
- [45] Lee, H. S. , Hwang, S.-J. , Kim, H. K. , Lee, Y.-S. , Park, J. , Yu, J.-S. , and Cho, Y. W. In Situ NMR Study on the Interaction between LiBH<sub>4</sub>-Ca(BH<sub>4</sub>)<sub>2</sub> and Mesoporous Scaffolds. *The Journal of Physical Chemistry Letters* **2012**, 3, 2922-2927.
- [46] Vitillo, J. , Bordiga, S. , and Baricco, M. Spectroscopic and Structural Characterization of Thermal Decomposition of  $\gamma$ -Mg(BH<sub>4</sub>)<sub>2</sub>: Dynamic Vacuum versus H<sub>2</sub> Atmosphere. *The Journal of Physical Chemistry C* **2015**, 119, 25340-25351.
- [47] Paskevicius, M. , Pitt, M. P. , Webb, C. J. , Sheppard, D. A. , Filsø, U. , Gray, E. M. , and Buckley, C. E. In-Situ X-ray Diffraction Study of  $\gamma$ -Mg(BH<sub>4</sub>)<sub>2</sub> Decomposition. *The Journal of Physical Chemistry C* **2012**, 116, 15231-15240.
- [48] Schouwink, P. , Ramel, A. , Giannini, E. , and Radovan, Ć. ESI Flux-assisted single crystal growth and heteroepitaxy of perovskite-type mixed-metal borohydrides. **2015**
- [49] Schouwink, P. , Ley, M. B. , Jensen, T. R. , Smrčok, L. , and Černý, R. Borohydrides: from sheet to framework topologies. *Dalton Transactions* **2014**, 43, 7726.
- [50] Kim, K. C. and Sholl, D. S. Crystal Structures and Thermodynamic Investigations of LiK(BH<sub>4</sub>)<sub>2</sub> , KBH<sub>4</sub> , and NaBH<sub>4</sub> from First-Principles Calculations. *The Journal of Physical Chemistry C* **2010**, 114, 678-686.
- [51] Poletti, M. G. and Battezzati, L. Electronic and thermodynamic criteria for the occurrence of high entropy alloys in metallic systems. *Acta Materialia* **2014**, 75, 297-306.

## Table of Contents

Ternary and quaternary equimolar mixture, synthesized by mechanochemical treatment, in the  $\text{LiBH}_4\text{-NaBH}_4\text{-KBH}_4\text{-Mg(BH}_4)_2\text{-Ca(BH}_4)_2$  system were experimentally investigated. The obtained phases were analysed by XRD, HP-DSC and DTA-MS. The investigation has evidenced the formation of bi/tri-metallic compounds such as  $\text{KCa(BH}_4)_3$ ,  $\text{LiKMg(BH}_4)_4$  and  $\text{LiK(BH}_4)_2$ , and many new eutectics. The relative thermodynamic stabilities of these compounds have been discussed. Hydrogen desorption occurs from the liquid phase, via complex multi-steps reactions but with no significant differences compared to the quinary equimolar mixture previously investigated.

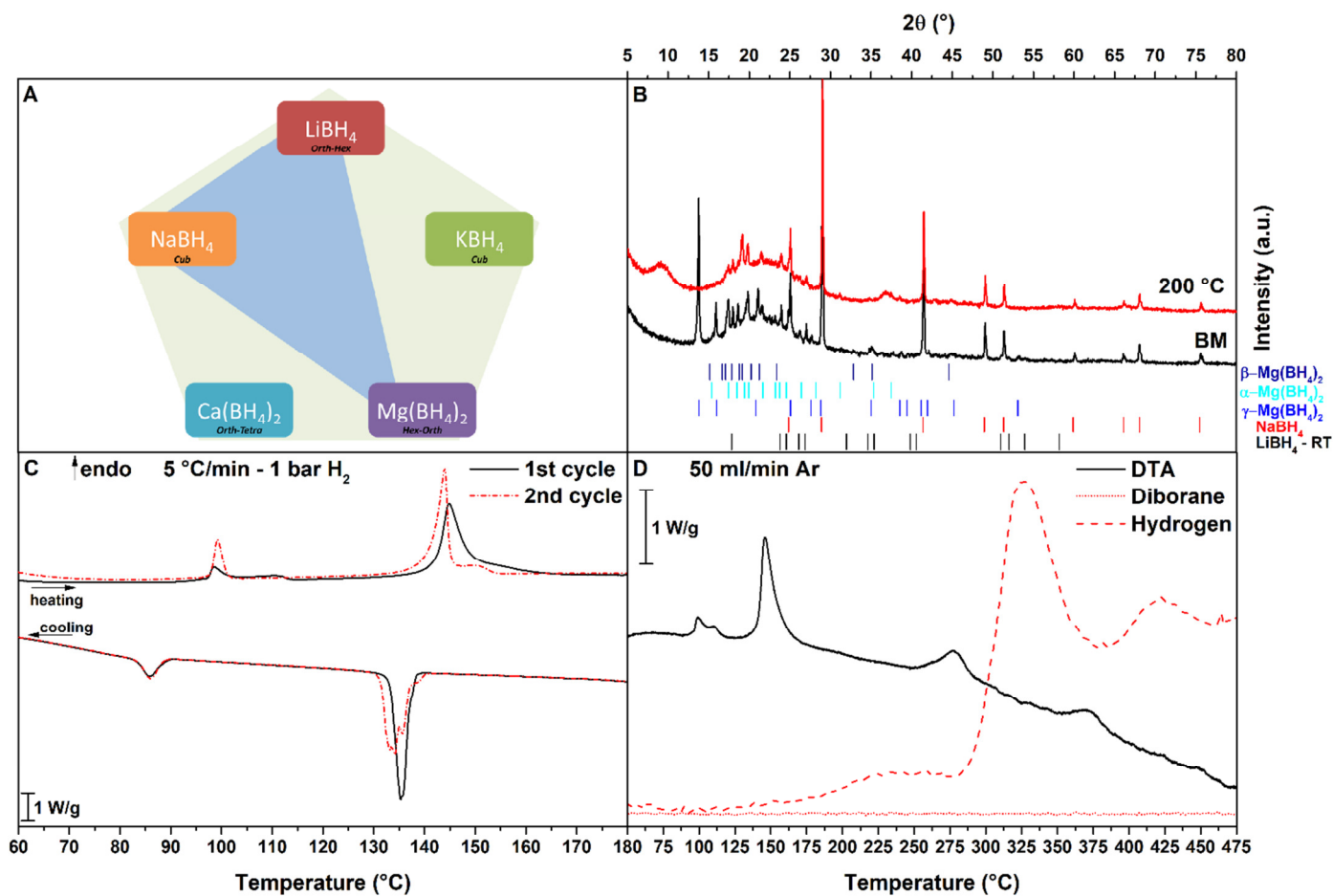


**Figure 1** – LiNaMg system: A) Schematic representation of the system, B) PXD pattern of BM and annealed sample, C) HP-DSC trace, 2 cycle of heating and cooling under 1 bar of  $\text{H}_2$ , D) DTA-MS analysis up to 500 °C under 50 ml/min of Ar. Heating rate equal to at 5 °C/min, endo up.

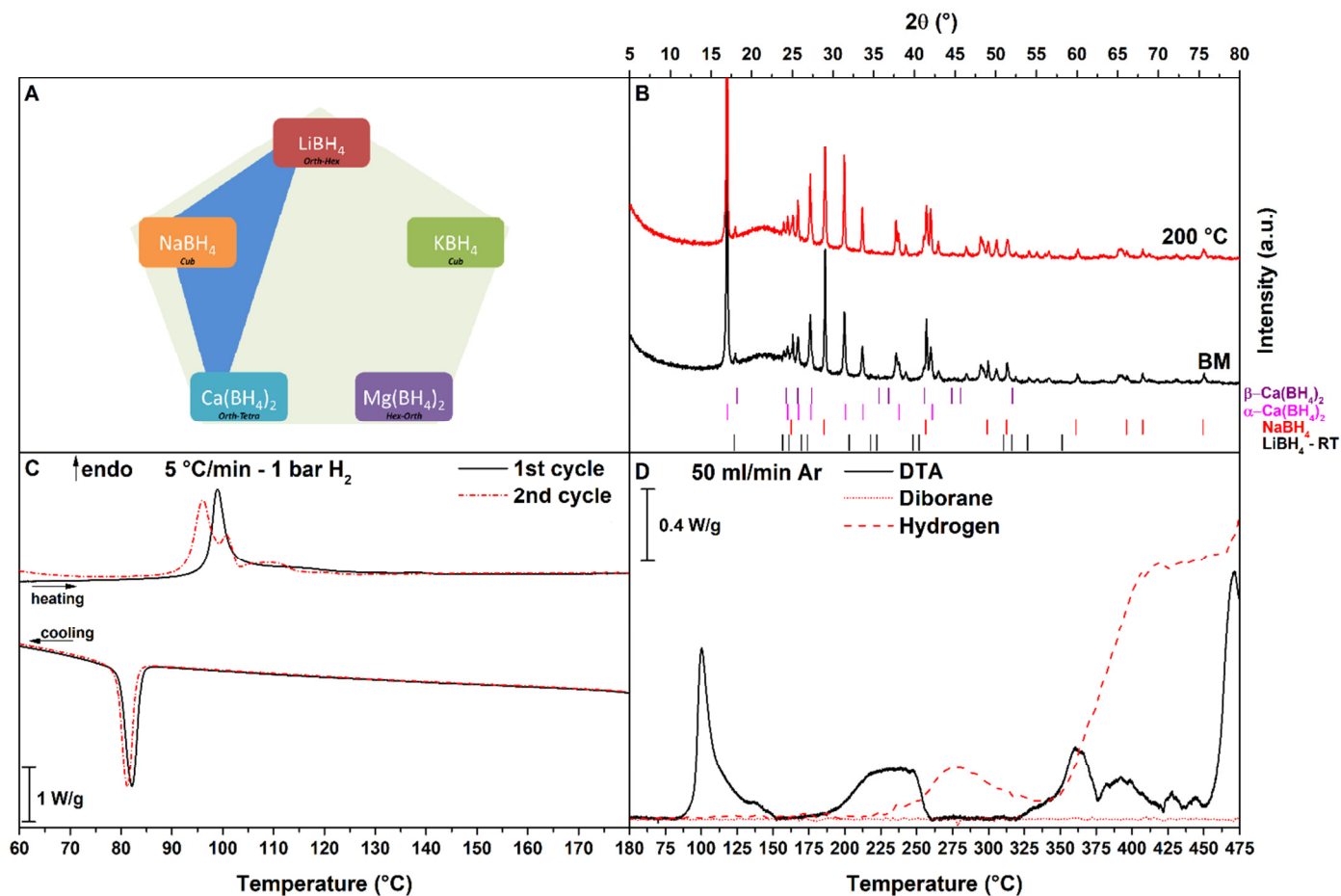


**Figure 2** – LiNaCa system: A) Schematic representation of the system, B) PXD pattern of BM and annealed sample, C) HP-DSC trace, 2 cycle of heating and cooling under 1 bar of  $H_2$ , D) DTA-MS analysis up to 500 °C under 50 ml/min of Ar. Heating rate equal to at 5 °C/min, endo up.

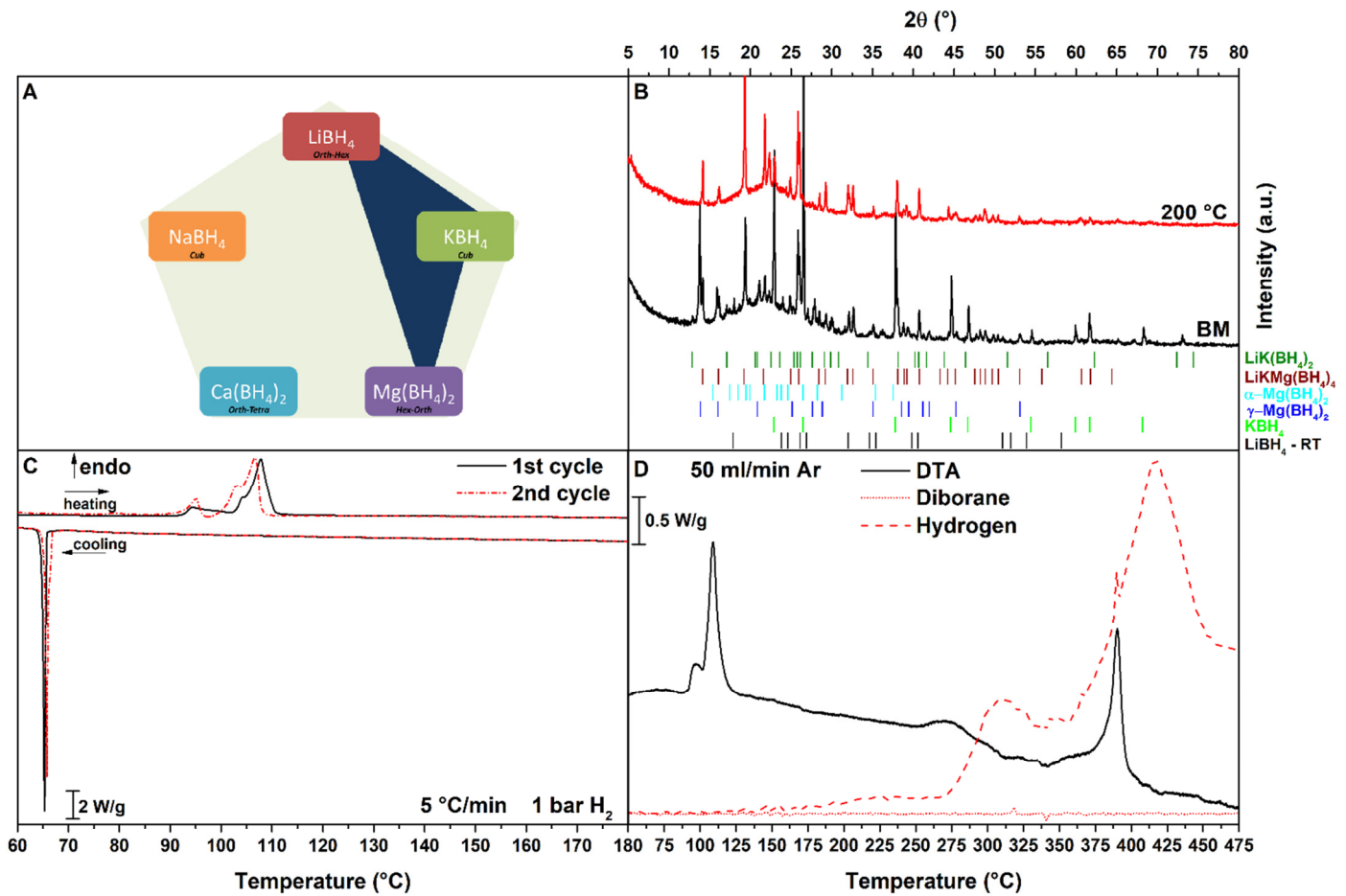


**Figure 3** – LiKMg system: A) Schematic representation of the system, B) PXD pattern of BM and annealed sample, C) HP-DSC trace, 2 cycle of heating and cooling under 1 bar of  $\text{H}_2$ , D) DTA-MS analysis up to  $500\text{ }^\circ\text{C}$  under  $50\text{ ml/min}$  of Ar. Heating rate equal to at  $5\text{ }^\circ\text{C}/\text{min}$ , endo up.

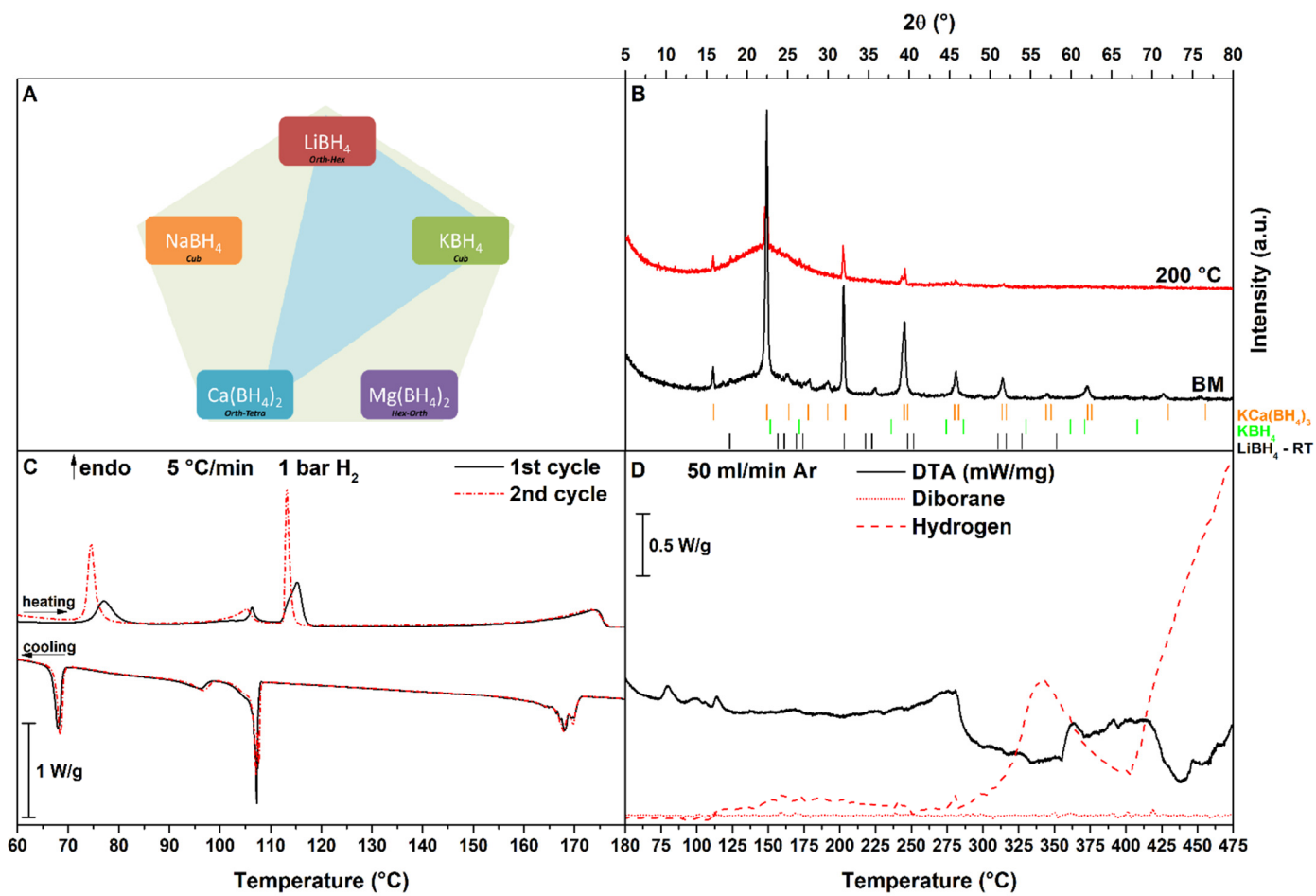


**Figure 4** – LiKCa system: A) Schematic representation of the system, B) PXD pattern of BM and annealed sample, C) HP-DSC trace, 2 cycle of heating and cooling under 1 bar of  $\text{H}_2$ , D) DTA-MS analysis up to  $500\text{ }^\circ\text{C}$  under  $50\text{ ml/min}$  of Ar. Heating rate equal to at  $5\text{ }^\circ\text{C/min}$ , endo up.

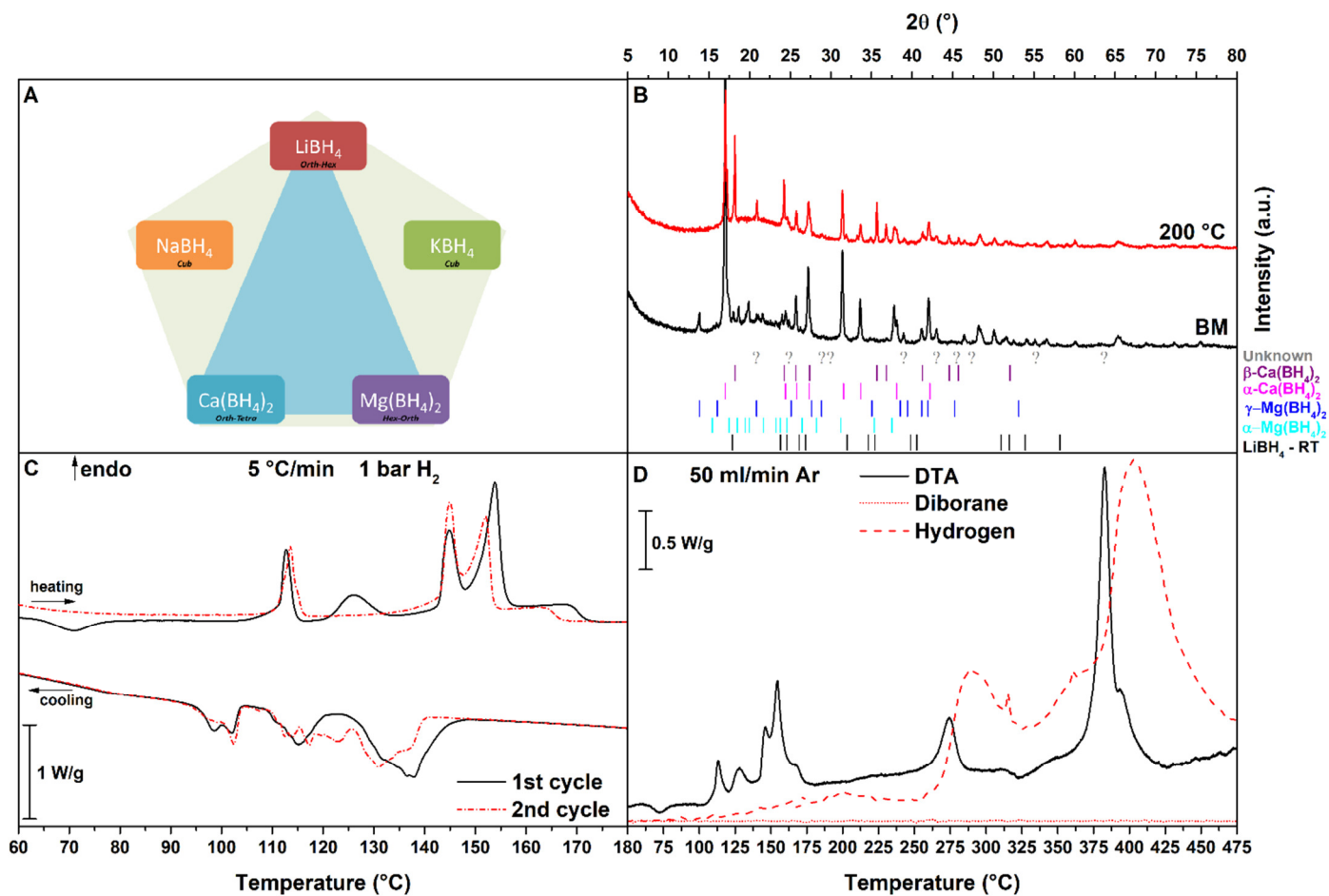


**Figure 5** – LiMgCa system: A) Schematic representation of the system, B) PXD pattern of BM and annealed sample, C) HP-DSC trace, 2 cycle of heating and cooling under 1 bar of  $\text{H}_2$ , D) DTA-MS analysis up to 500 °C under 50 ml/min of Ar. Heating rate equal to at 5 °C/min, endo up.



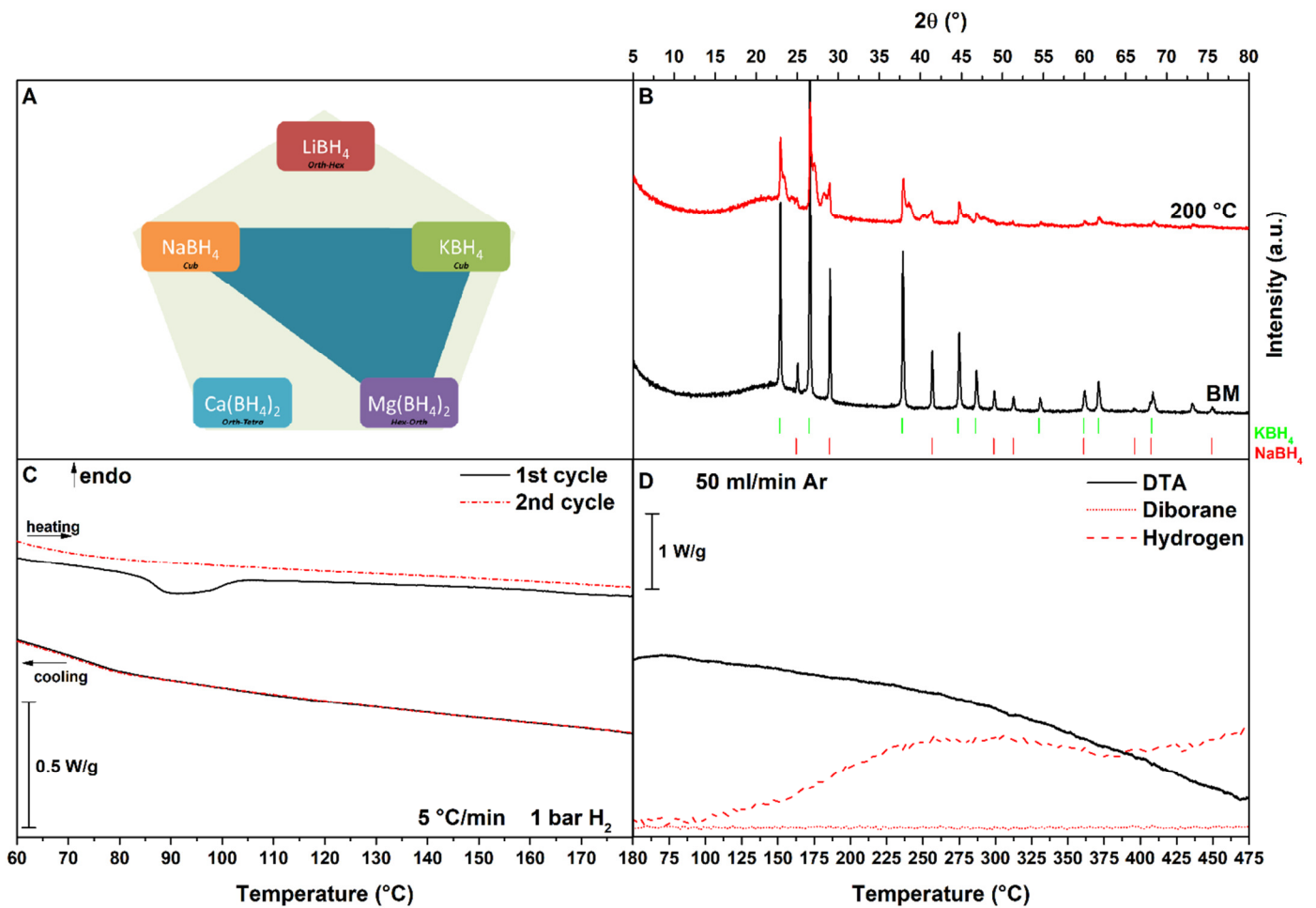


**Figure 6** – NaKMg system: A) Schematic representation of the system, B) PXD pattern of BM and annealed sample, C) HP-DSC trace, 2 cycle of heating and cooling under 1 bar of H<sub>2</sub>, D) DTA-MS analysis up to 500 °C under 50 ml/min of Ar. Heating rate equal to at 5 °C/min, endo up.

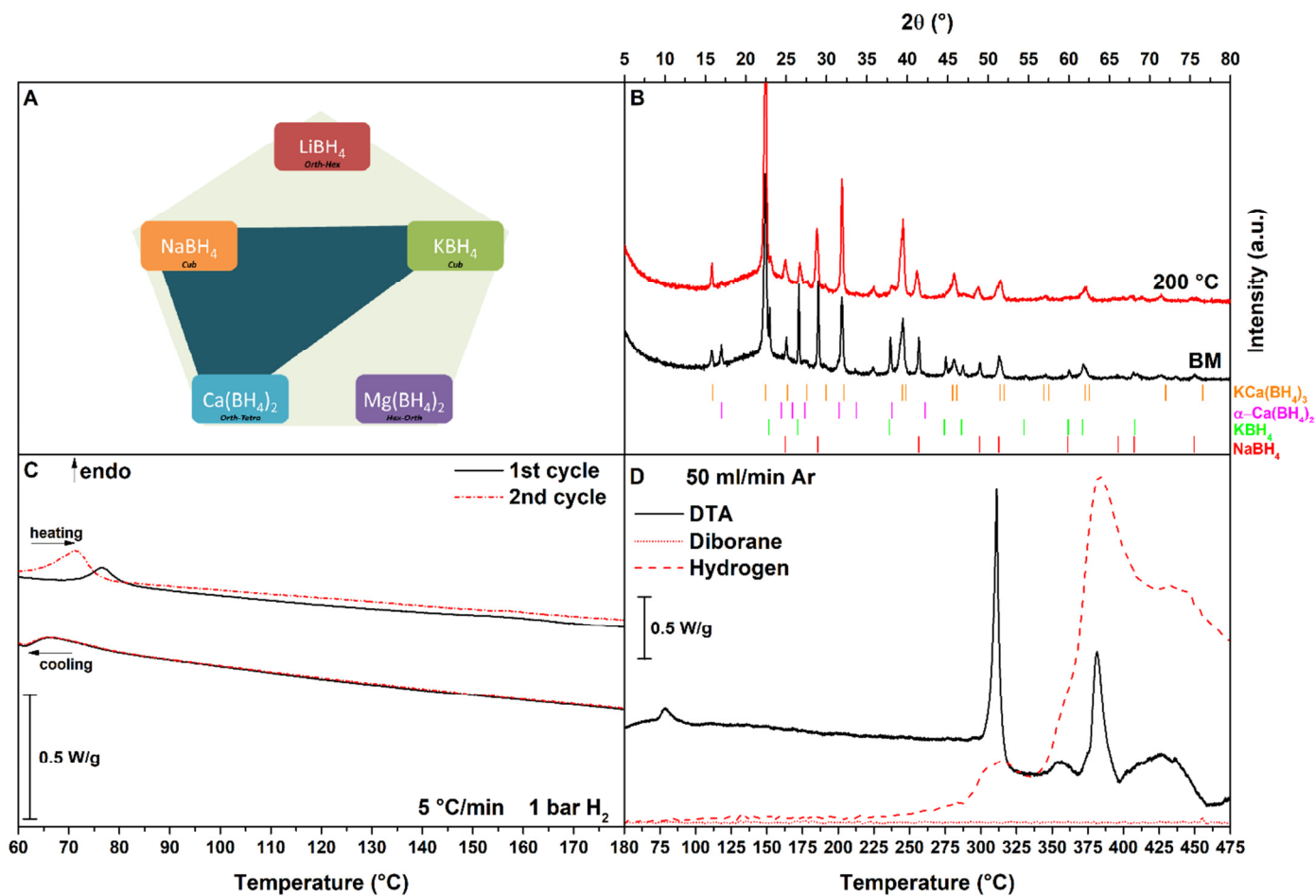


**Figure 7** – NaKCa system: A) Schematic representation of the system, B) PXD pattern of BM and annealed sample, C) HP-DSC trace, 2 cycle of heating and cooling under 1 bar of H<sub>2</sub>, D) DTA-MS analysis up to 500 °C under 50 ml/min of Ar. Heating rate equal to at 5 °C/min, endo up.

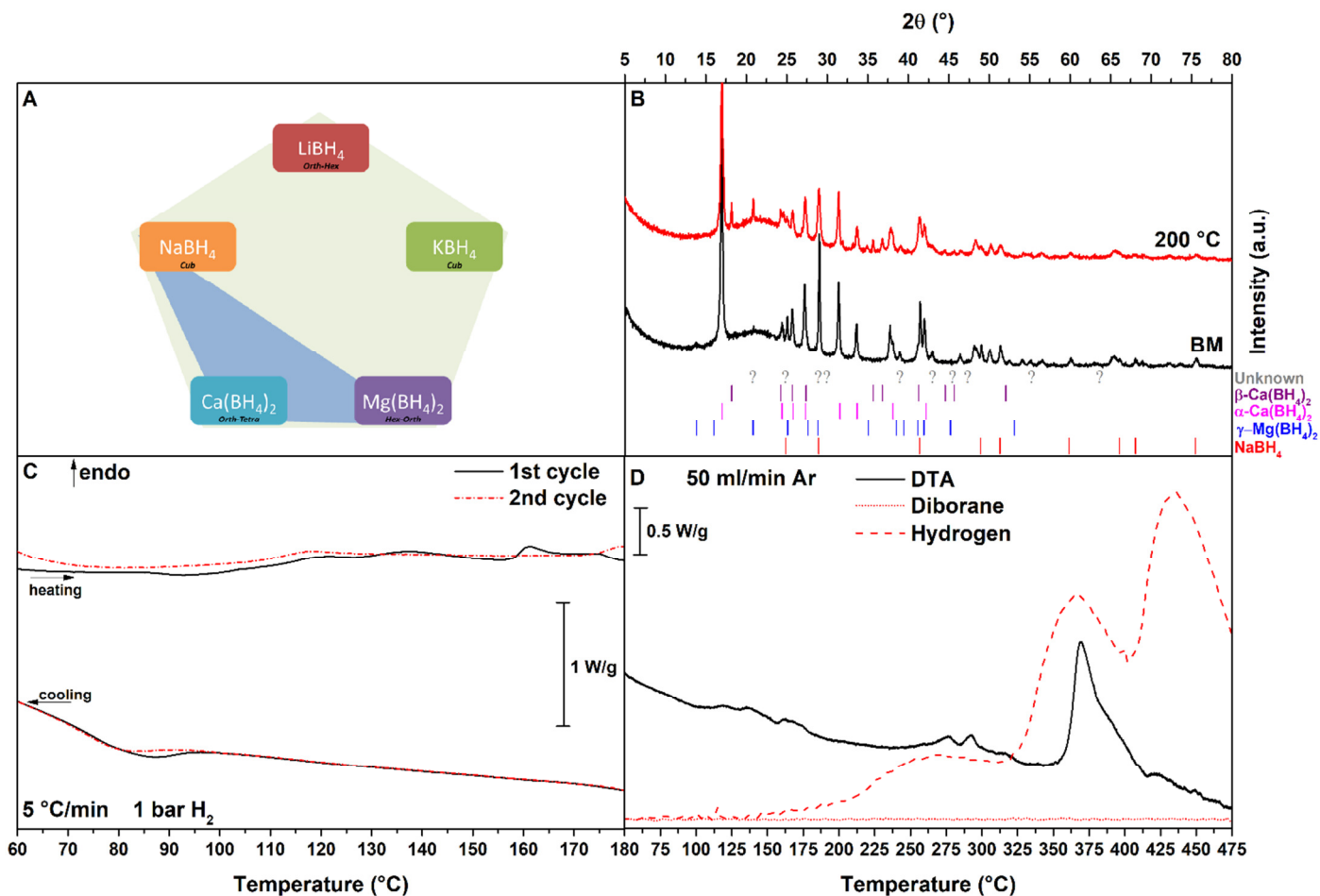


**Figure 8** – NaMgCa system: A) Schematic representation of the system, B) PXD pattern of BM and annealed sample, C) HP-DSC trace, 2 cycle of heating and cooling under 1 bar of  $\text{H}_2$ , D) DTA-MS analysis up to 500 °C under 50 ml/min of Ar. Heating rate equal to at 5 °C/min, endo up.

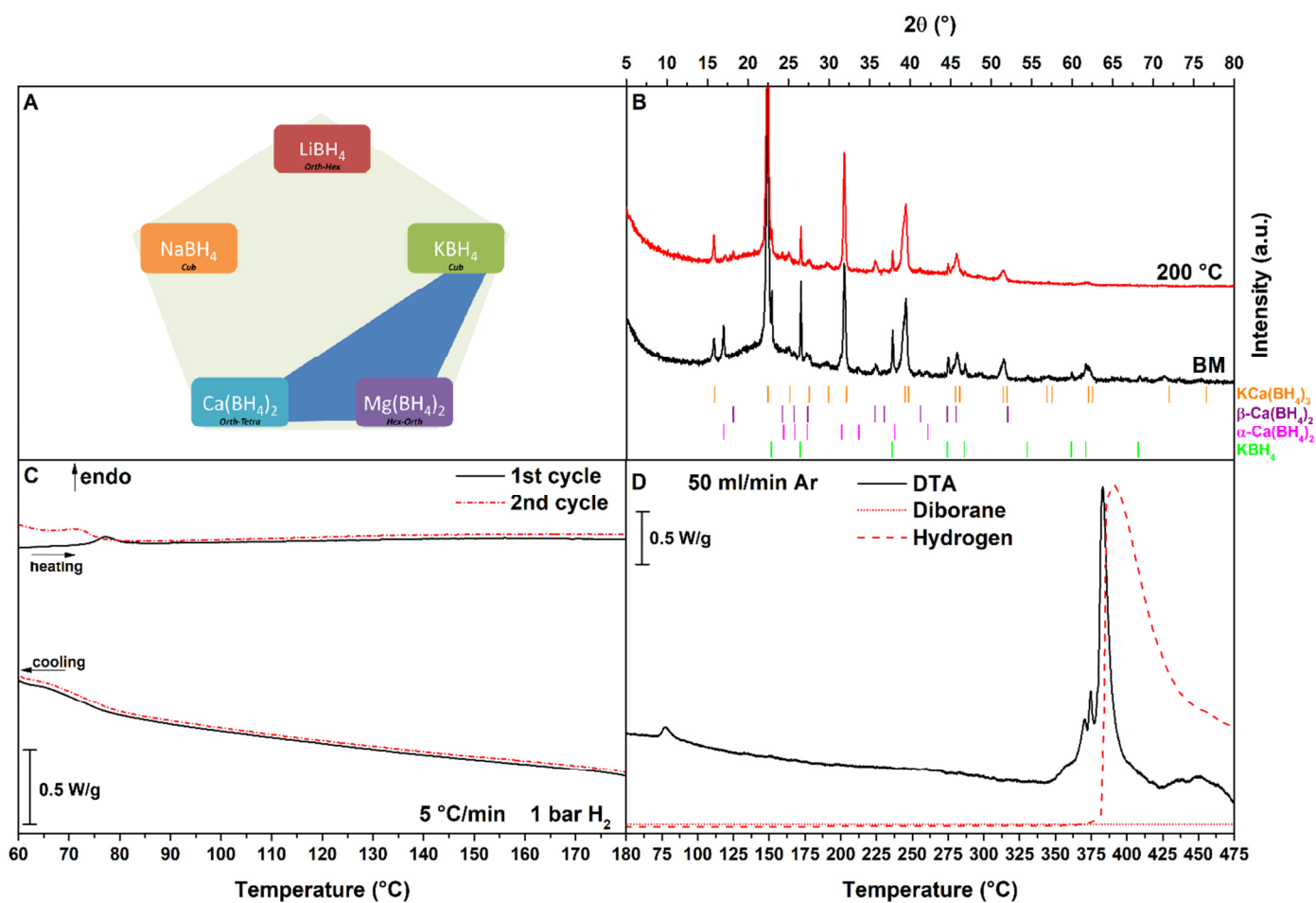


**Figure 9** – KMgCa system: A) Schematic representation of the system, B) PXD pattern of BM and annealed sample, C) HP-DSC trace, 2 cycle of heating and cooling under 1 bar of  $\text{H}_2$ , D) DTA-MS analysis up to 500 °C under 50 ml/min of Ar. Heating rate equal to at 5 °C/min, endo up.

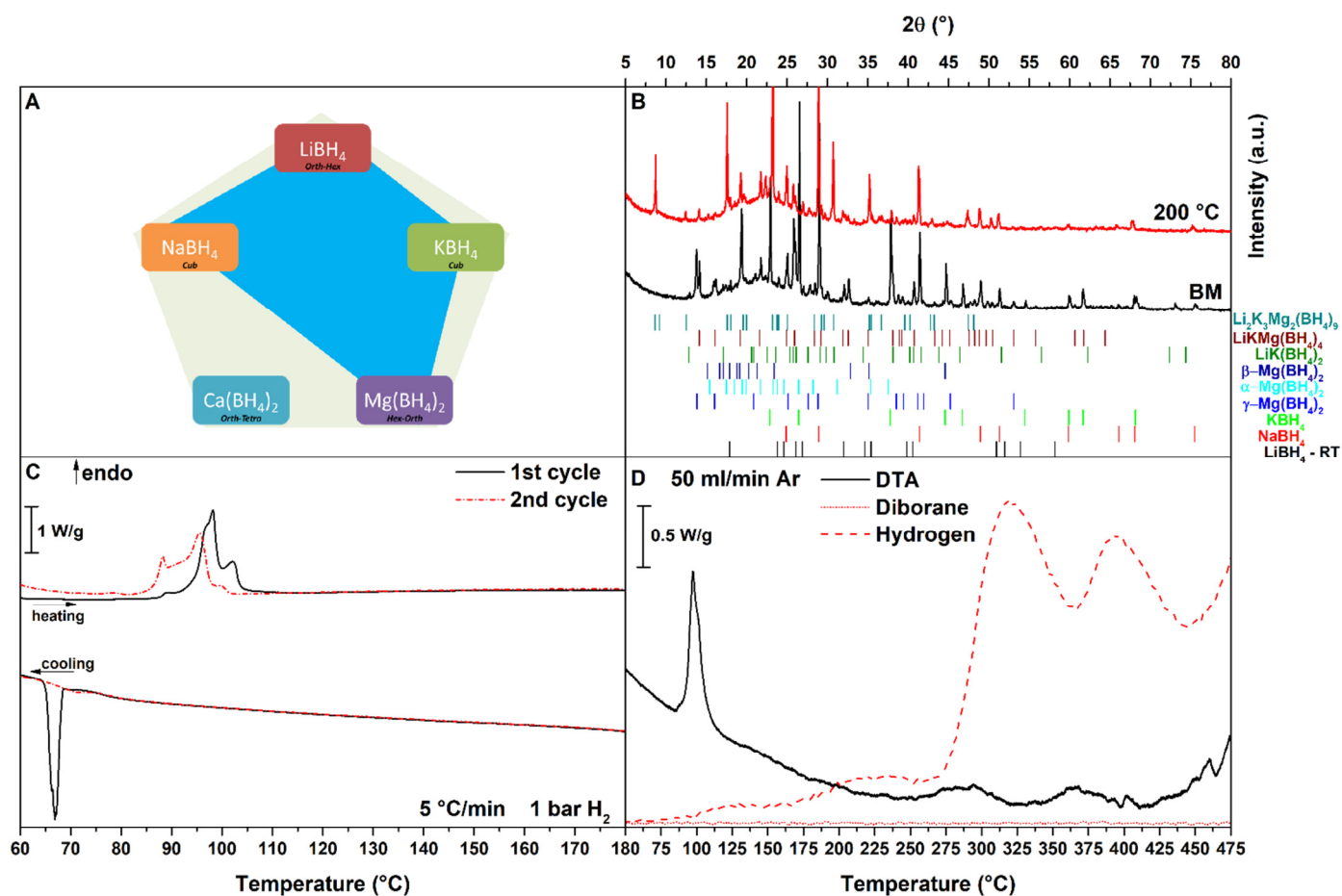


**Figure 10** – LiNaKMg system: A) Schematic representation of the system, B) PXD pattern of BM and annealed sample, C) HP-DSC trace, 2 cycle of heating and cooling under 1 bar of  $\text{H}_2$ , D) DTA-MS analysis up to 500 °C under 50 ml/min of Ar. Heating rate equal to at 5 °C/min, endo up.

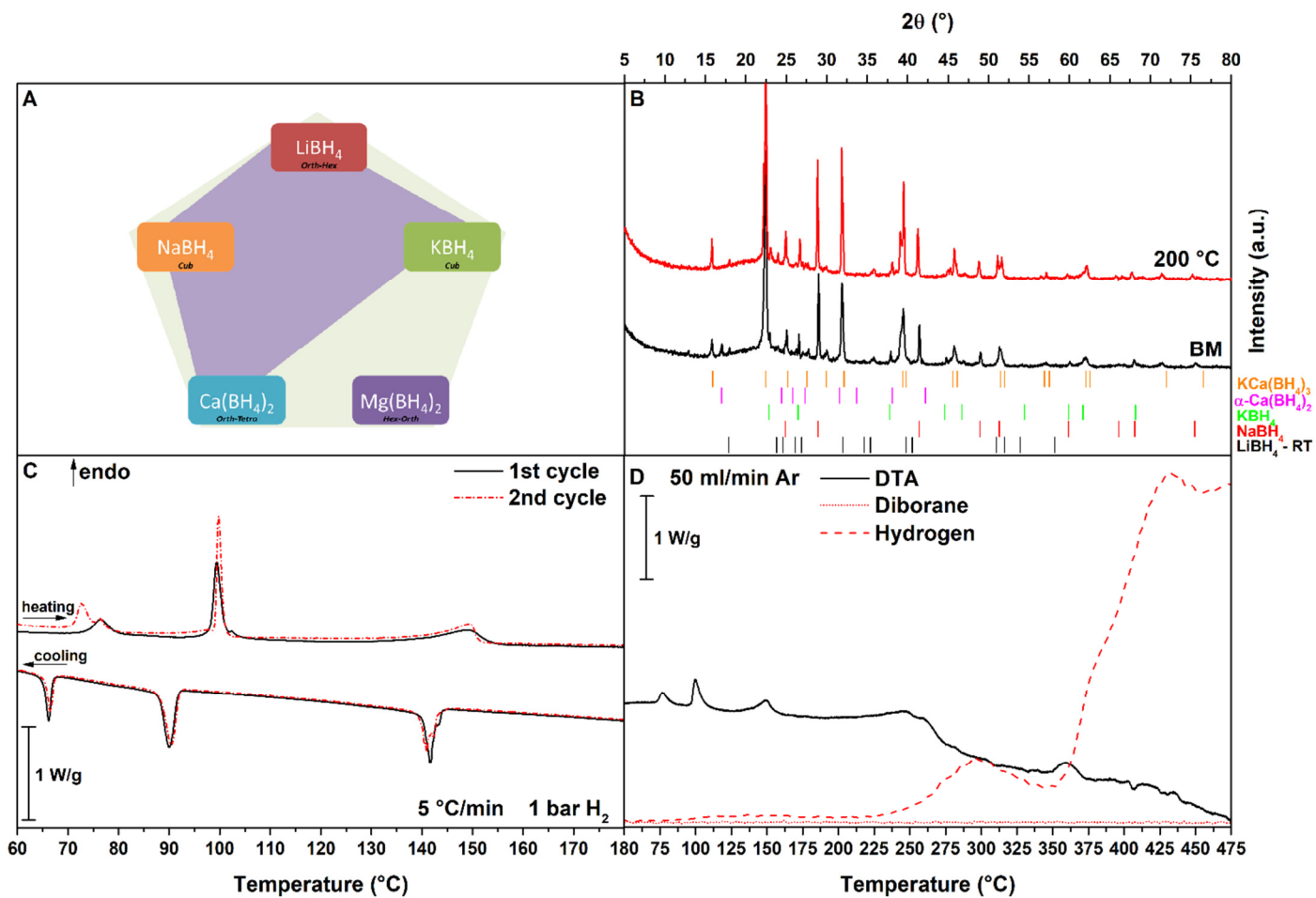


**Figure 11** – LiNaKCa system: A) Schematic representation of the system, B) PXD pattern of BM and annealed sample, C) HP-DSC trace, 2 cycle of heating and cooling under 1 bar of  $\text{H}_2$ , D) DTA-MS analysis up to  $500\text{ }^\circ\text{C}$  under  $50\text{ ml/min}$  of Ar. Heating rate equal to at  $5\text{ }^\circ\text{C/min}$ , endo up.

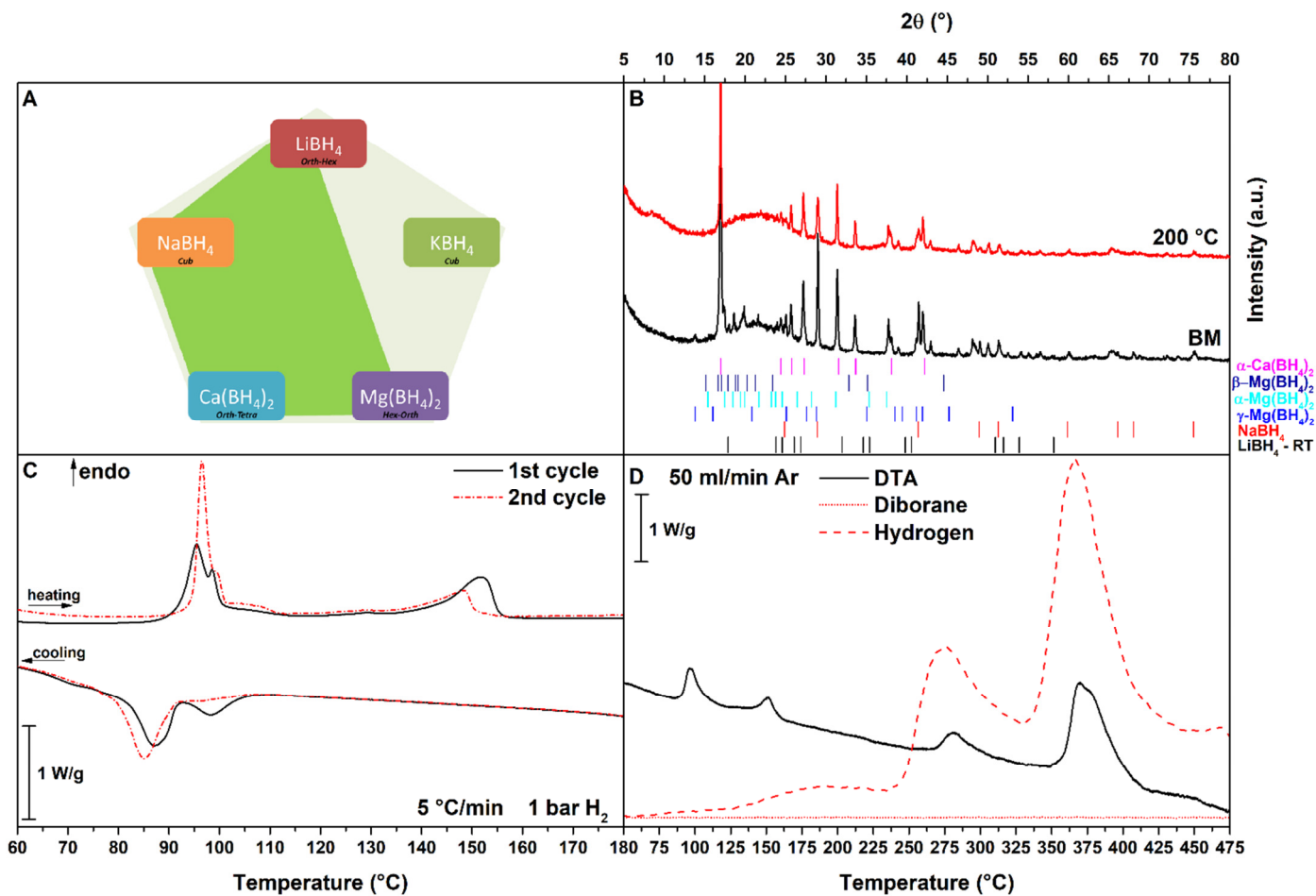


**Figure 12** – LiNaMgCa system: A) Schematic representation of the system, B) PXD pattern of BM and annealed sample, C) HP-DSC trace, 2 cycle of heating and cooling under 1 bar of  $\text{H}_2$ , D) DTA-MS analysis up to  $500\text{ }^\circ\text{C}$  under  $50\text{ ml/min}$  of Ar. Heating rate equal to at  $5\text{ }^\circ\text{C/min}$ , endo up.

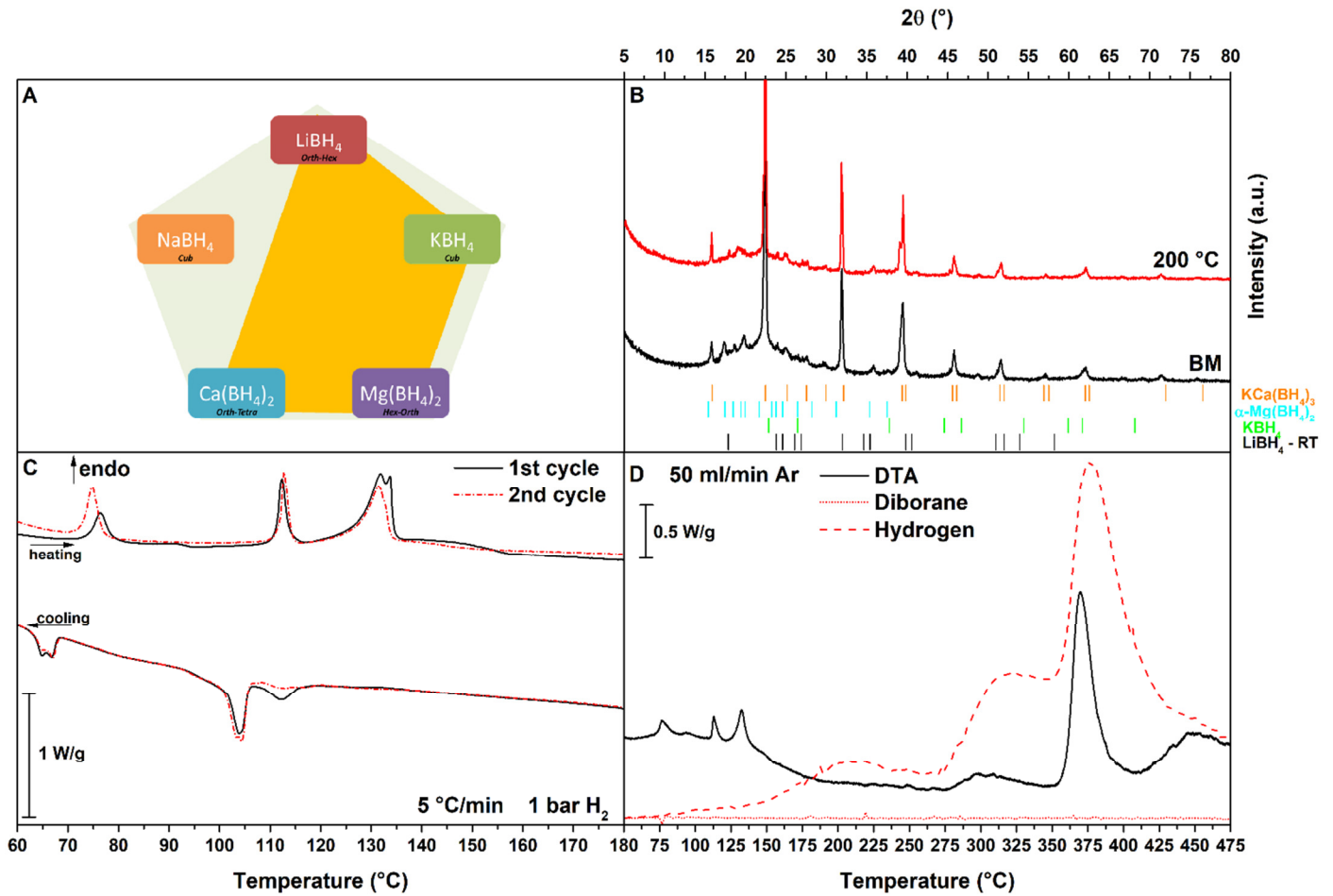


**Figure 13** – LiKMgCa system: A) Schematic representation of the system, B) PXD pattern of BM and annealed sample, C) HP-DSC trace, 2 cycle of heating and cooling under 1 bar of H<sub>2</sub>, D) DTA-MS analysis up to 500 °C under 50 ml/min of Ar. Heating rate equal to at 5 °C/min, endo up. Because of its small amount in PXD pattern, LiKMg(BH<sub>4</sub>)<sub>4</sub> tag is not reported in legend.



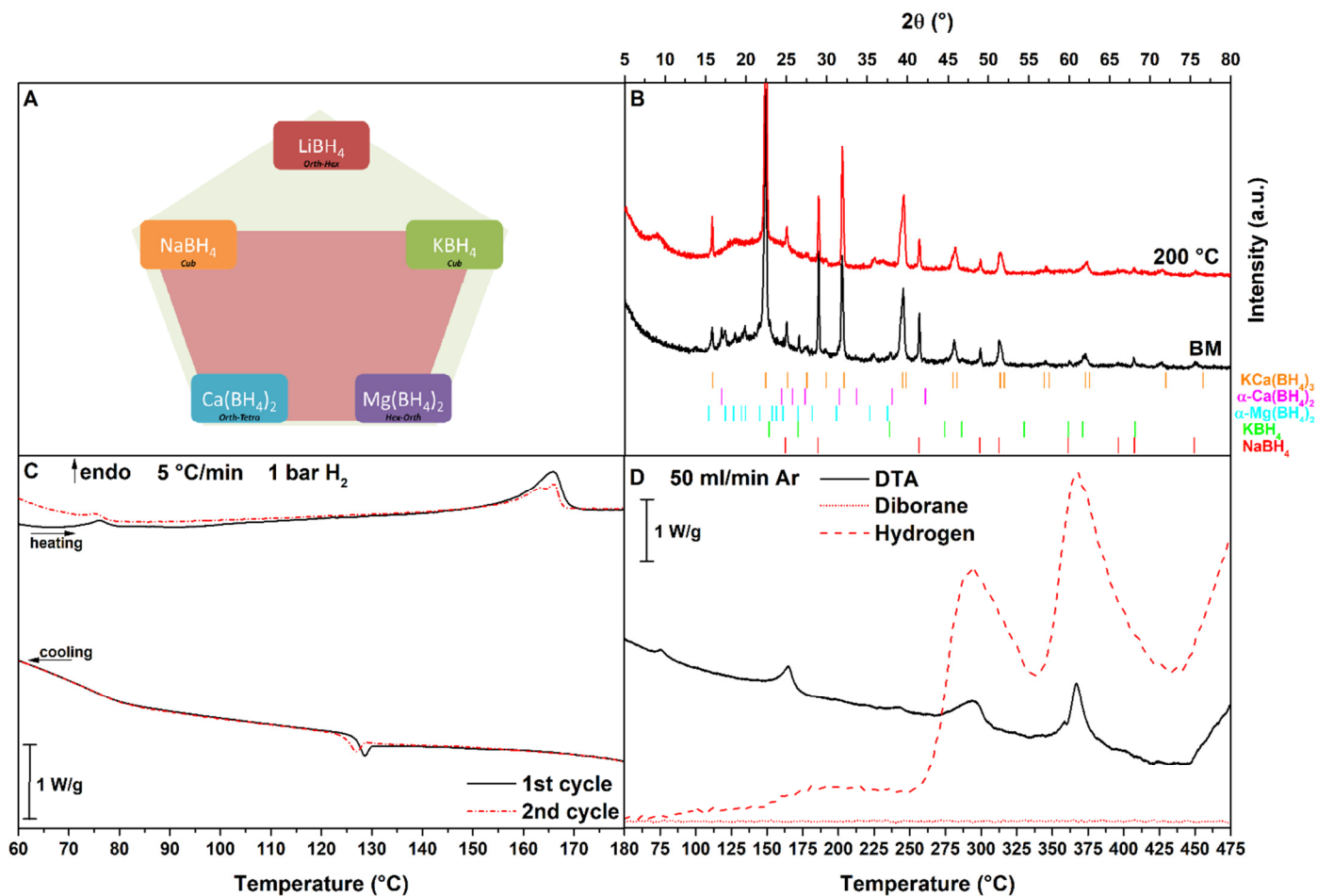


**Figure 14** – NaKMgCa system: A) Schematic representation of the system, B) PXD pattern of BM and annealed sample, C) HP-DSC trace, 2 cycle of heating and cooling under 1 bar of  $\text{H}_2$ , D) DTA-MS analysis up to 500 °C under 50 ml/min of Ar. Heating rate equal to at 5 °C/min, endo up.